MCD of Nonaromatic Cyclic π-Electron Systems. 3.[1] The Perimeter Model for Low-Symmetry "Unaromatic" and "Ambiaromatic" Molecules Derived from 4*N*-Electron [*n*]Annulenes

Jörg Fleischhauer,[†] Udo Höweler, and Josef Michl*,[‡]

Department of Chemistry and Biochemistry, University of Colorado, Boulder, Colorado 80309-0215

Received: January 7, 2000; In Final Form: May 2, 2000

The LCAO version of the perimeter model with overlap through second order is used to treat the $\pi\pi^*$ electronic absorption and magnetic circular dichroism (MCD) of low-symmetry molecules with a closed-shell ground state and no degenerate states (no threefold or higher order axis) derived from biradical (antiaromatic) parent 4*N*-electron [*n*]annulene perimeters by structural perturbations. If a symmetry plane perpendicular to the molecular plane is present, simple explicit algebraic solutions are obtained. Rules are derived for predicting the intensities, polarizations, and MCD signs of low-energy transitions in this class of molecules from the knowledge of relative magnitudes of MO energy differences, which can be frequently deduced by mere inspection of molecular formulas. On the basis of the results, a generalized nomenclature is proposed for low-energy electronic excited states of all even-electron cyclic π systems with a single perimeter.

Introduction

The present series of papers deals with a generalization of the LCAO version of the perimeter model for $\pi\pi^*$ states of cyclic π-electron systems. The original version of the model[2] applied to aromatic molecules, i.e., those derived from $(4N + 2)$-electron annulenes by structural perturbations such as cross-linking, bridging, bond length and bond angle distortions, substitutions, heteroatom replacement, etc. It accounted for trends in their transition energies, intensities, and polarizations and classified the low-energy excited singlet states as G, L_b, L_a, B_b, B_a (uncharged perimeters). A subsequent extension of the model to the treatment of magnetic circular dichroism (MCD)[3,4,5] also involved a generalization to aromatic systems derived from charged perimeters,[3] whose states were classified as G, L_1, L_2, B_1, and B_2. Even though it is possible nowadays to perform quite accurate ab initio calculations even for large π-electron systems and account for numerous states of a single molecule, we believe that simple models capable of correlating the low-energy states of many structurally related molecules have not lost their value, as they permit an intuitive understanding of trends and of results of large-scale numerical calculations.

The present elaboration of the model extends it to the other large class of closed-shell cyclic π-electron systems, those derived from 4*N*-electron [*n*]annulenes.[6,7] In part 1[8] we developed the theory for the singlet states of unperturbed high-symmetry (D_{nh}) parent [*n*]annulenes and those cyclic π-electron systems derivable from these perimeters that still have degenerate or nearly degenerate frontier orbitals (SOMO) and are perfect or nearly perfect biradicals. In the nomenclature that we use for the purposes of discussion of electronic and MCD spectra,[8] such "open-shell" ground state molecules are referred to as "antiaromatic" (their frontier orbital one-electron energies are split by $\Delta S < 2[2N]$, where the value of the electron repulsion integral $[2N]$ depends on *n* and typically is of the order of 1 eV, cf. Figure 3 of part 1[8]).

Part 2[1] and the present part 3 of this series are dedicated to the practically more important π-electron systems that can be formally derived from a 4*N*-electron [*n*]annulene by symmetry-lowering perturbations strong enough to change the ground state from a perfect biradical to a biradicaloid or an ordinary closed-shell species. As discussed in detail in part 2,[1] this requires the one-electron part of the frontier orbital (SOMO) splitting ΔS to be equal to at least $2[2N]$, which is on the order of 2 eV. We refer to such closed-shell ground state π systems as "unaromatic". Closed-shell ground systems that can be equally well derived from a $(4N + 2)$-electron and a 4*N*-electron perimeter are called "ambiaromatic". Unfortunately, electronic states of unaromatic and ambiaromatic molecules derived from an uncharged perimeter do not correlate unambiguously with those of their antiaromatic parents, because of the presence of conical intersections in the space spanned by structural perturbations.

In part 2,[1] we developed the general theory and then worked out in detail the results for spectroscopic properties of high-symmetry unaromatic and ambiaromatic molecules, i.e., those possessing a threefold or higher order symmetry axis. We found general rules for the properties of transitions from the ground (G) to four $\pi\pi^*$ excited singlet states, S, D, N, and P. The quantity that controls the spectral behavior is a difference of two orbital energy gaps, called ΔHSL. Qualitatively, it reflects the relative energies of excitation of electrons and holes from the half-occupied "Fermi" level. The first two of the four $\pi\pi^*$ excited states are nondegenerate and transitions into them are forbidden, whereas the last two are doubly degenerate and give rise to symmetry-allowed transitions. Transitions into the N state are weak, and those into the higher energy P state are intense.

We now describe similar but more complicated results for lower symmetry molecules. In these, degeneracies are removed, and six excited states result: S, D, N_α, N_β, P_α, and P_β. Explicit algebraic solutions for the absorption and MCD spectral properties of transitions from the G state to these six states can

[†] Permanent address: Institut für Organische Chemie, RWTH Aachen, Prof.-Pirlet-Str. 1, D-52056 Aachen, Germany.

[‡] This project was initiated at the University of Utah.

10.1021/jp000116h CCC: $19.00
Published on Web 07/29/2000

be obtained as long as at least one symmetry plane perpendicular to the molecular plane is present. In addition to the quantity ΔHSL, two additional orbital energy differences, ΔH and ΔL, now play an important role in determining the spectral behavior.

Certain π systems derived from $4N$-electron perimeters have a reduced number of states in the perimeter model and require a separate treatment (cf. part 1[8]): (i) $N = 1$, such as $C_3H_3^-$, C_4H_4, $C_5H_5^+$, $C_6H_6^{2+}$, and, in general, $C_nH_n^{n-4}$, (ii) $N = n/2 - 1$ (n even) or $N = (n - 1)/2$ (n odd), such as $C_6H_6^{2-}$ and, in general, $C_nH_n^{4-n}$ (n even) or $C_nH_n^{2-n}$ (n odd). The procedure is the same as outlined below for the general case and need not be described explicitly.

Finally, we consider in some detail the issue of state correlation within the families of aromatic and nonaromatic cyclic π-electron systems and propose a general nomenclature for their low-energy electronic states.

Results and Discussion

Outline. The reader is referred to parts 1[8] and 2[1] for the detailed formulation of the perimeter model for $4N$-electron [n]-annulenes. Here, we only summarize the main features and general results briefly and proceed to work out the results for the specific case of lower symmetry molecules. Subsequently, in part 4,[9] we shall consider the explicit relations between molecular structure and spectra and shall illustrate the application of the general results to two specific molecules, acenaphthylene and pleiadiene. Both of these are ambiaromatic, and their excited states have already been labeled and MCD spectra analyzed in terms of the rules valid for the classical $(4N + 2)$-electron perimeter model.[10] In part 4,[9] we examine the alternative state labeling in terms of the $4N$-electron perimeter model and derive the same observed MCD signs from the different set of rules applicable in this case.

In subsequent papers of this series, we plan to report and analyze the MCD spectra of several families of unaromatic cyclic π-electron systems in terms of the simple model developed in parts 1−4.

AO Basis. For the π system of a parent D_{nh} $4N$-electron [n]-annulene,[8] n nonorthogonal $2p_z$ atomic orbitals labeled 0 to $n - 1$ are located at the vertices of a regular polygon. Its center lies at the origin of a right-handed coordinate system spanned by unit vectors $\boldsymbol{x}$, $\boldsymbol{y}$, and $\boldsymbol{z}$. The x axis passes through atom 0, and z is perpendicular to the polygon. The AOs are subject to an explicit Löwdin orthogonalization, considering overlap integrals only through second order. In the orthogonal basis of orbitals χ_ν, only the nearest-neighbor resonance integrals β_1 are kept in the evaluation of energy terms and the zero-differential-overlap approximation[11] is adopted.

MO Basis. The energy of the complex MOs

$$\psi_k = n^{-1/2}\sum_{\nu=0}^{n-1}[\exp(2\pi ik\nu/n)]\chi_\nu \tag{1}$$

grows with increasing $|k|$, $k = 0, \pm1, ..., \pm(n - 1)/2$ for n odd, or $\pm n/2$ for n even (but then, $\psi_{n/2} = \psi_{-n/2}$).

The only nonvanishing matrix elements of the one-electron electric ($\hat{\boldsymbol{m}}$) and magnetic ($\hat{\boldsymbol{\mu}}$) dipole moment operators in the MO basis are

$$\langle\psi_k|\hat{\boldsymbol{m}}|\psi_{k\pm1}\rangle = m(n, |2k \pm 1|)(\boldsymbol{x} \pm i\boldsymbol{y})/\sqrt{2} \tag{2}$$
$$\langle\psi_k|\hat{\boldsymbol{\mu}}|\psi_k\rangle = -\langle\psi_{-k}|\hat{\boldsymbol{\mu}}|\psi_{-k}\rangle = \mu(n, k)\boldsymbol{z}, \quad k > 0$$

Their values are simple functions of n and k.[3]

Molecular Orbitals of Perturbed Perimeters. In the lowest three singlet configurations of a general n-atom $4N$-electron perimeter, all MOs up to ψ_{N-1} and ψ_{-N+1} (the HO pair) are doubly occupied, the MOs ψ_N and ψ_{-N} (SO pair) hold a total of two electrons, and ψ_{N+1}, ψ_{-N-1} (the LO pair) as well as all higher MOs are empty.

In the unperturbed perimeter, the one-electron parts of the energies of the three important orbital pairs are $E(\mathrm{HO}) = E(\psi_{N-1}) = E(\psi_{-N+1})$, $E(\mathrm{SO}) = E(\psi_N) = E(\psi_{-N})$, and $E(\mathrm{LO}) = E(\psi_{N+1}) = E(\psi_{-N-1})$. A symmetry-lowering perturbation that preserves at most D_{2h} symmetry will cause all degenerate orbital levels to split. Presently, we treat low-symmetry perturbed annulenes that do not possess a symmetry axis of order higher than two and whose SO orbital pair is split strongly enough to produce a closed-shell ground state. As before, we consider only the one-electron part of the structural perturbation, represent it by the operator $\hat{a}$, and treat only the mixing of originally degenerate orbitals.

The effect of a perturbation $\hat{a}$ on the energies of a pair of degenerate complex perimeter MOs with "magnetic quantum numbers" k and $-k$ is described by two quantities: the diagonal element k_D and the off-diagonal element $k_0e^{i\varkappa}$, responsible for the mutual one-to-one mixing of the two degenerate orbitals ($0 \le \varkappa \le 2\pi$, k_0, $k > 0$):

$$k_D = \langle\psi_k|\hat{a}|\psi_k\rangle = \langle\psi_{-k}|\hat{a}|\psi_{-k}\rangle$$
$$k_0e^{i\varkappa} = \langle\psi_k|\hat{a}|\psi_{-k}\rangle \tag{3}$$

The real MOs $\psi_+(k)$ and $\psi_-(k)$ are

$$\psi_+(k) = (e^{i\varkappa/2}\psi_k + e^{-i\varkappa/2}\psi_{-k})/\sqrt{2}$$
$$\psi_-(k) = (-ie^{i\varkappa/2}\psi_k + ie^{-i\varkappa/2}\psi_{-k})/\sqrt{2} \tag{4}$$

and their energies are

$$E[\psi_+(k)] = E(\psi_k) + k_D + k_0$$
$$E[\psi_-(k)] = E(\psi_k) + k_D - k_0 \tag{5}$$

such that $E[\psi_+(k)] \ge E[\psi_-(k)]$.

The MOs given in eq 4 serve as a one-electron basis for the seven configuration state functions used below (cf. part 2[1]). We adopt the following labels for the members of the HO, SO, and LO pairs:

$$h_\pm = \psi_\pm(N - 1)$$
$$s_\pm = \psi_\pm(N)$$
$$l_\pm = \psi_\pm(N + 1) \tag{6}$$

In the general case, we use $k_\pm = \psi_\pm(k)$.

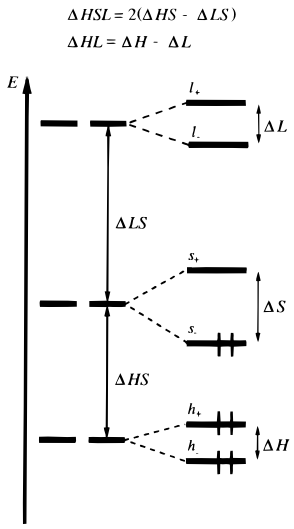

Figure 1. Definition of ΔH, ΔS, ΔL, ΔHL, and ΔHSL in terms of orbital energies.

Perturbation Characteristics. In first-order perturbation molecular orbital (PMO[12]) theory, structural perturbations are defined by the parameters ΔH, ΔS, ΔL, ΔHL, ΣHL, and ΔHSL (Figure 1):

$$\Delta H = E(h_+) - E(h_-) = 2h_0 \geq 0$$

$$\Delta S = E(s_+) - E(s_-) = 2s_0 \geq 0 \tag{7}$$

$$\Delta L = E(l_+) - E(l_-) = 2l_0 \geq 0$$

$$\Delta HL = \Delta H - \Delta L$$

$$\Sigma HL = \Delta H + \Delta L \tag{8}$$

$$\Delta HSL = \{[E(s_+) + E(s_-) - E(h_+) - E(h_-)] - [E(1_+) + E(1_-) - E(s_+) - E(s_-)]\}$$
$$= 2[2E(\mathrm{SO}) - E(\mathrm{HO}) - E(\mathrm{LO}) + 2s_\mathrm{D} - h_\mathrm{D} - l_\mathrm{D}] \tag{9}$$

For unaromatic and ambiaromatic molecules, ΔS must be larger than $2[2N]$, i.e., at least 2 eV. The differences ΔHL and ΔHSL can be positive, zero, or negative. The quantity ΔHSL is only affected by the diagonal part of the perturbation k_D ($k = h, s, l$) and reflects the relative size of (i) the separation of the average energy of the two MOs that result from the HO pair of the perimeter from the average energy of the two MOs that result from the SO pair and (ii) the similar separation of the LO and SO pairs. In practice, the differences of one-electron energies of the MOs h_-, h_+, s_-, s_+, l_-, and l_+ do not need to be obtained from first-order perturbation theory, although this is usually the simplest and quite adequate way. Frequently, it is convenient to obtain their relative differences from Hückel theory. If a better approximation is needed, semiempirical or ab initio computed MO energies that include electron repulsion terms can be used, since for the symmetry-determined perimeter orbitals the ΔH, ΔL, and ΔHSL values are nearly the same (for uncharged perimeters, exactly the same) regardless of whether one-electron (core) or full orbital energies are used for their evaluation (for ΔH, the difference is $2\delta_{-2q}[2N]\cos(\eta + \sigma)$; for ΔL, it is $2\delta_{2q}[2N]\cos(\lambda + \sigma)$; and for ΔHSL, it is $[2N+1] - [2N-1]$, using the symbols introduced in part 1;[8] see also below). The differences of full orbital energies can also be obtained from differences of energies of singly excited configurations: $E(\Psi^{l+}_{s-}) - E(\Psi^{l-}_{s-})$, $E(\Psi^{s+}_{h-}) - E(\Psi^{s+}_{h+})$, and $E(\Psi^{s+}_{h-}) + E(\Psi^{s+}_{h+}) - E(\Psi^{l+}_{s-}) - E(\Psi^{l-}_{s-})$, respectively (see below). Although this procedure is equivalent for the original perimeter orbitals, it may give somewhat different results when using the results of calculations on the real molecules. In cases of doubt, it is probably preferable, since after all, it is the composition of state wave functions of the real molecule in terms of configurations contributing opposed contributions to transition moments that determines the signs of the magnetic mixing terms in MCD.

The perturbation parameters can also be obtained from experimental values of ionization potentials and electron affinities, using Koopmans' theorem. The value of ΔS, for which the two-electron contributions do not cancel properly, cannot be obtained in this way, but it is actually not needed for the prediction of MCD B terms. We shall see below that ΔS equals $[E(\Psi^{s+,s+}_{s-,s-}) - E(\Psi_\mathrm{R})]/2$, and at least in principle could be estimated from the observed energy of the lowest doubly excited state.

The phase factor $\varkappa$ that appears in eqs 3 and 4 completes the description of the structural perturbation for our purposes. It is related to the angles of complex rotation that have to be applied to the complex MOs ψ_k and ψ_{-k} in order for the resulting real MOs to be adapted to the perturbation. This rotation places the nodal points in the resulting real MOs into the positions dictated by the perturbation. We use $\varkappa$ for the phase angle that describes the effect of a perturbation on a general degenerate complex MO pair ψ_k, ψ_{-k}. For the HO pair ψ_{N-1}, ψ_{-N+1}, we use the symbol η, for the SO pair ψ_N, ψ_{-N}, we use σ, and for the LO pair ψ_{N+1}, ψ_{-N-1}, we use λ.

The value of $\varkappa$ depends on the atom numbering choice, and we choose a numbering that minimizes $|\sigma|$. We shall find below that relatively simple explicit solutions for spectroscopic observables can only be obtained if the molecule possesses a plane of symmetry perpendicular to the molecular plane. If this plane passes through an atom, we give this atom the label 0, and only the angles $\varkappa = 0$ or $\varkappa = \pi$ are then possible. If the plane cuts through the midpoint of a bond, the label 0 is assigned to an atom on this bond located counterclockwise from the midpoint, and only the angles $\varkappa = 2\pi k/n$ or $\varkappa = 2\pi k/n - \pi$ are possible (if n is even, there may be two symmetry planes and the choice between them is arbitrary). The value of $\varkappa$ can be deduced from the symmetry of the orbital k_- relative to reflection in the symmetry plane, as described below.

Configuration State Functions. In the lowest energy configuration Ψ_R that serves as a reference for the CI space, the MOs are doubly occupied through the h_-, h_+, and s_- levels. Six singlet excited configuration state functions describe the lowest energy one-electron excitations within the HO−SO and SO−LO range and the lowest energy doubly excited configuration $s_-^2 \rightarrow s_+^2$. We use the notation Ψ^l_k for the configuration state function that results from a singlet excitation from ψ_k to ψ_l. In part 2,[1] we expressed these configuration state functions

in terms of the initial complex orbitals; equivalent expressions in terms of the real orbitals are

$$\Psi_R = |...h_-^2\ h_+^2\ s_-^2\rangle$$

$$\Psi_{s-}^{s+} = 2^{-1/2}(|...h_-^2\ h_+^2\ s_-\bar{s}_+\rangle + |...h_-^2\ h_+^2\ s_+\bar{s}_-\rangle)$$

$$\Psi_{s-,s-}^{s+,s+} = |...h_-^2\ h_+^2\ s_+^2\rangle$$

$$\Psi_{s-}^{l-} = 2^{-1/2}(|...h_-^2\ h_+^2\ s_-\bar{l}_-\rangle + |...h_-^2\ h_+^2\ l_-\bar{s}_-\rangle) \quad (10)$$

$$\Psi_{s-}^{l+} = 2^{-1/2}(|...h_-^2\ h_+^2\ s_-\bar{l}_+\rangle + |...h_-^2\ h_+^2\ l_+\bar{s}_-\rangle)$$

$$\Psi_{h+}^{s+} = -2^{-1/2}(|...h_-^2\ h_+\bar{s}_+s_-^2\rangle + |...h_-^2\ s_+\bar{h}_+s_-^2\rangle)$$

$$\Psi_{h-}^{s+} = -2^{-1/2}(|...h_-\bar{s}_+h_+^2\ s_-^2\rangle + |...s_+\bar{h}_-h_+^2\ s_-^2\rangle)$$

These seven real configuration state functions are used for the description of the ground and the lowest few excited states of the systems in which the splitting of the SO level is large enough for Ψ_R to represent well the ground-state wave function ($\Delta S > 2[2N]$). The additional 4 configurations that can be constructed from the 11 initial complex configurations are doubly excited with respect to the reference configuration Ψ_R and are not used. They carry no intensity in ordinary absorption and MCD spectra if Ψ_R is a good representation of the ground state and would not affect these spectra at all in the absence of configuration mixing.

In some π systems with a relatively small ΔS gap, such as pentalene and heptalene, one or two of the doubly excited configurations are calculated to lie low enough in energy to intrude into the range of the states described presently by the perimeter model. The presence of each such "intruder" configuration results in an increase of the number of excited states in the region, but unless they are accidentally nearly degenerate with one of those already present in the model, the resulting intruder state will carry very little absorption and MCD intensity. If such doubly excited intruder states are calculated to be present, we shall give them the label of that perimeter state with which they mix the most and distinguish them with a prime (e.g., N'_α). Their actual observation in ordinary absorption or MCD spectra is infrequent.

The configurations used here are not related simply to those of aromatic systems derived from $(4N + 2)$-electron perimeters, which lead to L and B states in the standard Platt nomenclature[2] for aromatics. For example, in a perturbed $4N$-electron system, a transition to the lowest energy configuration Ψ_{s-}^{s+} describes an excitation within an orbital pair that arises from the splitting of the complex MOs ψ_N and ψ_{-N}, possessing the same absolute value $|N|$ of the magnetic quantum number ("intrashell" excitation), and thus is magnetic dipole allowed, but carries no electric dipole oscillator strength. To the contrary, the superficially analogous lowest energy configuration Ψ_{HOMO}^{LUMO} of a perturbed $(4N + 2)$-electron system, which dominates either the lower or the upper L state in Platt's notation, describes an excitation from an orbital arising from ψ_N and ψ_{-N} into an orbital arising from ψ_{N+1} and ψ_{-N-1} ("intershell" excitation) and thus is magnetic dipole forbidden and electric dipole allowed (except in certain high-symmetry cases). It is therefore not appropriate to characterize the excited states of systems derived from $4N$-electron perimeters, such as ordinary quinones, in terms of Platt's notation.

Matrix Elements between Configuration State Functions. The nonvanishing matrix elements of the total magnetic dipole moment operator $\hat{M}$ in the real configuration basis are

$$\langle\Psi_R|\hat{M}|\Psi_{s-}^{s+}\rangle = \langle\Psi_{s-}^{s+}|\hat{M}|\Psi_{s-,s-}^{s+,s+}\rangle = i\sqrt{2}\mu(n, N)\boldsymbol{z}$$

$$\langle\Psi_{s-}^{l-}|\hat{M}|\Psi_{s-}^{l+}\rangle = i\mu(n, N+1)\boldsymbol{z} \quad (11)$$

$$\langle\Psi_{h+}^{s+}|\hat{M}|\Psi_{h-}^{s+}\rangle = -i\mu(n, N-1)\boldsymbol{z}$$

We use the notation introduced in part 1:[8]

$$\mu_\pm = \mu(n, N+1) \pm \mu(n, N-1) \quad (12)$$

$$\mu = \mu(n, N) \quad (13)$$

This differs from the definition of $\mu^\pm$ used with $(4N + 2)$-electron perimeters.[3] Like μ^+, μ_+ is large and negative, and like μ^-, μ_- is much smaller, negative for positively charged or neutral perimeters and positive for strongly negatively charged ones. For numerical values, see part 2.[1]

The nonvanishing matrix elements of the total electric dipole moment operator $\hat{\boldsymbol{M}}$ are

$$\langle\Psi_R|\hat{\boldsymbol{M}}|\Psi_{s-}^{l-}\rangle = m(n, 2N+1)\boldsymbol{e}_{\lambda 1}$$

$$\langle\Psi_R|\hat{\boldsymbol{M}}|\Psi_{s-}^{l+}\rangle = -m(n, 2N+1)\boldsymbol{e}_{\lambda 2}$$

$$\langle\Psi_R|\hat{\boldsymbol{M}}|\Psi_{h+}^{s+}\rangle = -m(n, 2N-1)\boldsymbol{e}_{\eta 1}$$

$$\langle\Psi_R|\hat{\boldsymbol{M}}|\Psi_{h-}^{s+}\rangle = m(n, 2N-1)\boldsymbol{e}_{\eta 2}$$

$$\langle\Psi_{s-}^{s+}|\hat{\boldsymbol{M}}|\Psi_{s-}^{l-}\rangle = (1/\sqrt{2})m(n, 2N+1)\boldsymbol{e}_{\lambda 2}$$

$$\langle\Psi_{s-}^{s+}|\hat{\boldsymbol{M}}|\Psi_{s-}^{l+}\rangle = (1/\sqrt{2})m(n, 2N+1)\boldsymbol{e}_{\lambda 1} \quad (14)$$

$$\langle\Psi_{s-}^{s+}|\hat{\boldsymbol{M}}|\Psi_{h+}^{s+}\rangle = (1/\sqrt{2})m(n, 2N-1)\boldsymbol{e}_{\eta 2}$$

$$\langle\Psi_{s-}^{s+}|\hat{\boldsymbol{M}}|\Psi_{h-}^{s+}\rangle = (1/\sqrt{2})m(n, 2N-1)\boldsymbol{e}_{\eta 1}$$

$$\boldsymbol{e}_{\lambda 1} = \boldsymbol{x}\cos[(\lambda - \sigma)/2] - \boldsymbol{y}\sin[(\lambda - \sigma)/2]$$

$$\boldsymbol{e}_{\lambda 2} = \boldsymbol{x}\sin[(\lambda - \sigma)/2] + \boldsymbol{y}\cos[(\lambda - \sigma)/2]$$

$$\boldsymbol{e}_{\eta 1} = \boldsymbol{x}\cos[(\sigma - \eta)/2] - \boldsymbol{y}\sin[(\sigma - \eta)/2]$$

$$\boldsymbol{e}_{\eta 2} = \boldsymbol{x}\sin[(\sigma - \eta)/2] + \boldsymbol{y}\cos[(\sigma - \eta)/2]$$

The negative quantities $m(n, 2N - 1)$ and $m(n, 2N + 1)$ were introduced in parts 1[8] and 2[1] and ref 3. We use the notation

$$m^+ = m(n, 2N+1)$$

$$m^- = m(n, 2N-1) \quad (15)$$

$$m_\pm \equiv m^+ \pm m^- = m(n, 2N+1) \pm m(n, 2N-1)$$

All nonvanishing matrix elements of $\hat{\boldsymbol{M}}$ that involve the seven configuration state functions in question are comparable in magnitude. They come in pairs polarized in mutually perpendicular directions, given by $\boldsymbol{e}_{\lambda 1}$, $\boldsymbol{e}_{\lambda 2}$, or $\boldsymbol{e}_{\eta 1}$, $\boldsymbol{e}_{\eta 2}$ for transition pairs involving excitations into l_-, l_+ or from h_+, h_-, respectively. These directions are rotated by $(\lambda - \sigma)/2$ and $(\sigma - \eta)/2$, respectively, with respect to the initial system $\boldsymbol{x}$, $\boldsymbol{y}$, and

CHART 1: Matrix 16

	Ψ_R	Ψ_{s-}^{s+}	$\Psi_{s-,s-}^{s+,s+}$
Ψ_R	$E(\Psi_R)$	$-\delta_{0q}([2N]/\sqrt{2})\sin 2\sigma$	$([2N]/2)(1-\delta_{0q}\cos 2\sigma)$
Ψ_{s-}^{s+}	$-\delta_{0q}([2N]/\sqrt{2})\sin 2\sigma$	$E(\Psi_{s-}^{s+})$	$\delta_{0q}([2N]/\sqrt{2})\sin 2\sigma$
$\Psi_{s-,s-}^{s+,s+}$	$([2N]/2)(1-\delta_{0q}\cos 2\sigma)$	$\delta_{0q}([2N]/\sqrt{2})\sin 2\sigma$	$E(\Psi_{s-,s-}^{s+,s+})$

(16)

CHART 2: Matrix 17

	Ψ_{s-}^{l-}	Ψ_{s-}^{l+}	Ψ_{h+}^{s+}	Ψ_{h-}^{s+}
Ψ_{s-}^{l-}	$E(\Psi_{s-}^{l-})$	$-[([2N]+[2N+1])/2]\delta_{+2q}\sin(\lambda+\sigma)$	$-c^-$	s^+
Ψ_{s-}^{l+}	$-[([2N]+[2N+1])/2]\delta_{+2q}\sin(\lambda+\sigma)$	$E(\Psi_{s-}^{l+})$	$-s^+$	$-c^-$
Ψ_{h+}^{s+}	$-c^-$	$-s^+$	$E(\Psi_{h+}^{s+})$	$[([2N]+[2N+1])/2]\delta_{-2q}\sin(\sigma+\eta)$
Ψ_{h-}^{s+}	s^+	$-c^-$	$[([2N]+[2N+1])/2]\delta_{-2q}\sin(\sigma+\eta)$	$E(\Psi_{h-}^{s+})$

(17)

the polarization directions depend on the phase angles of the MO perturbations, as in the familiar case of perturbed $(4N+2)$-electron annulenes.[4]

Configuration Energies and Mixing. Except in the case of singly charged perimeters ($q = n - 4N = \pm 1$), the Hamiltonian matrix for perturbed $4N$-electron annulenes is block diagonal in the basis of singlet configurations Ψ_R, Ψ_{s-}^{s+}, $\Psi_{s-,s-}^{s+,s+}$, Ψ_{s-}^{l-}, Ψ_{s-}^{l+}, Ψ_{h+}^{s+}, and Ψ_{h-}^{s+}. It consists of a 3×3 matrix 16 (Chart 1) that yields the ground-state G, the lowest singly excited state S, and the lowest doubly excited state D (cf. ref 13), and a 4×4 matrix 17, from which the four higher singly excited states result (Chart 2) and where

$$c^- = (^1/_2)[1]\cos\rho^- - (^1/_2)\delta_{0q}[2N-1]\cos\rho^+$$

$$s^+ = (^1/_2)[1]\sin\rho^- + (^1/_2)\delta_{0q}[2N-1]\sin\rho^+ \qquad (18)$$

$$\rho^\pm = \sigma \pm (\eta+\lambda)/2$$

and δ_{iq} is the Kronecker delta. The electron repulsion integrals $[k]$ are those of part 1.[8] The nonvanishing two-electron repulsion integrals are those in which the overlap density due to one of the electrons transforms like ϵ_l, while that due to the other transforms like ϵ_{-l}. In the zero-differential overlap approximation, the magnitude of each integral depends only on $|l|$ and we write it as $[l]$. The integrals are positive and decrease in magnitude with increasing l from $l = 0$ to $l = n/2$ or $(n-1)/2$. Here and elsewhere, k is counted modulo n. In the presence of a plane of symmetry, $\delta_{+2q}\sin(\lambda+\sigma) = \delta_{-2q}\sin(\sigma+\eta) = 0$, and four of the off-diagonal elements in the 4×4 matrix vanish.

For singly charged perimeters, the 7×7 CI matrix is not block diagonal. The 3×3 and 4×4 blocks now interact through a 4×3 matrix 19 that contains only electron repulsion terms (Chart 3). The energies of the configurations are

$$E(\Psi_R) = E(\Psi_{-N}^N) - \Delta S + [2N]/2 + (^1/_2)\delta_{0q}[2N]\cos 2\sigma$$

$$E(\Psi_{s-}^{s+}) = E(\Psi_{-N}^N) - \delta_{0q}[2N]\cos 2\sigma$$

$$E(\Psi_{s-,s-}^{s+,s+}) = E(\Psi_R) + 2\,\Delta S = E(\Psi_{-N}^N) + \Delta S + [2N]/2 + (^1/_2)\delta_{0q}[2N]\cos 2\sigma$$

$$E(\Psi_{s-}^{l-}) = E(\Psi_{-N}^N) + c + (l_D - h_D)/2 - \Delta S/2 + ([1] + [2N+1])/2 + (\delta_{+2q}/2)([2N]+[2N+1])\cos(\lambda+\sigma) - \Delta HSL/4 - \Delta L/2$$

$$E(\Psi_{s-}^{l+}) = E(\Psi_{-N}^N) + c + (l_D - h_D)/2 - \Delta S/2 + ([1] + [2N+1])/2 - (\delta_{+2q}/2)([2N]+[2N+1])\cos(\lambda+\sigma) - \Delta HSL/4 + \Delta L/2$$

$$E(\Psi_{h+}^{s+}) = E(\Psi_{-N}^N) + c + (l_D - h_D)/2 - \Delta S/2 + ([1] + [2N-1])/2 + (\delta_{-2q}/2)([2N]+[2N-1])\cos(\eta+\sigma) + \Delta HSL/4 - \Delta H/2$$

$$E(\Psi_{h-}^{s+}) = E(\Psi_{-N}^N) + c + (l_D - h_D)/2 - \Delta S/2 + ([1] + [2N-1])/2 - (\delta_{-2q}/2)([2N]+[2N-1])\cos(\eta+\sigma) + \Delta HSL/4 + \Delta H/2 \qquad (20)$$

where $E(\Psi_{-N}^N)$ is the energy[8] of the perturbed complex configuration Ψ_{-N}^N.

The quantity c has the meaning introduced for the unperturbed systems in part 1.[8] It is characteristic of a parent perimeter and provides a measure of the separation of the LO and HO levels and thus an approximation to the energy difference between the intershell excited states resulting from the diagonalization of the 4×4 matrix and the intrashell excited states resulting from the diagonalization of the 3×3 matrix:

$$c = [E(\mathrm{LO}) - E(\mathrm{HO})]/2 + [1] - [2N] \qquad (21)$$

Since in practice c tends to be large and the energy of the ground state lies far below the energies of the four intershell excited states that result from the 4×4 matrix, the effect of the nonvanishing 3×4 matrix in the case of singly charged perimeters is small and shall be neglected.

The matrix element $\langle\psi_k|\hat{a}|\psi_k\rangle$ of the perturbing operator dictates the diagonal elements in eq 17, while the complex phase of $\langle\psi_k|\hat{a}|\psi_{-k}\rangle$ dominates the off-diagonal elements ($k = N-1$, N, $N+1$). This is quite unlike the familiar case of aromatic $(4N+2)$-electron perimeters.[4]

State Eigenfunctions and Spectroscopic Observables. The diagonalization of the Hamiltonian matrix produces the seven state eigenfunctions that need to be substituted into the general expressions[14] for A, B, and C terms, which characterize an MCD

CHART 3: Matrix 19

	Ψ_R	Ψ_{s-}^{s+}	$\Psi_{s-,s-}^{s+,s+}$
Ψ_{s-}^{l-}	$\delta_{+1q}([2N]/\sqrt{2})\cos[(\lambda+3\sigma)/2]$	$-\delta_{+1q}[2N]\sin[(\lambda+3\sigma)/2]$	$-\delta_{+1q}([2N]/\sqrt{2})\cos[(\lambda+3\sigma)/2]$
Ψ_{s-}^{l+}	$-\delta_{+1q}([2N]/\sqrt{2})\sin[(\lambda+3\sigma)/2]$	$-\delta_{+1q}[2N]\cos[(\lambda+3\sigma)/2]$	$\delta_{+1q}([2N]/\sqrt{2})\sin[(\lambda+3\sigma)/2]$
Ψ_{h+}^{s+}	$\delta_{-1q}([2N]/\sqrt{2})\cos[(\eta+3\sigma)/2]$	$-\delta_{-1q}[2N]\sin[(\eta+3\sigma)/2]$	$-\delta_{-1q}([2N]/\sqrt{2})\cos[(\eta+3\sigma)/2]$
Ψ_{h-}^{s+}	$\delta_{-1q}([2N]/\sqrt{2})\sin[(\eta+3\sigma)/2]$	$-\delta_{-1q}[2N]\cos[(\eta+3\sigma)/2]$	$-\delta_{-1q}([2N]/\sqrt{2})\sin[(\eta+3\sigma)/2]$

(19)

TABLE 1: Low-Symmetry Perturbed 4*N*-Electron [*n*]Annulenes ($\Delta S > 2[2N]$, ΔH, $\Delta L \neq 0$): State Energies (E) and Eigenfunctions[a]

state	E	wave function
G	$\epsilon(\Psi_R) - ([2N]/2)\tan\alpha\,[1 + \delta_{0q}(\delta_{\sigma,\pm\pi/2} - \delta_{\sigma,0} - \delta_{\sigma,\pi})]$	$\Psi(G) = \Psi_R \cos\alpha - \Psi^{s+,s+}_{s-,s-} \sin\alpha$
S	$[2N]\delta_{0q}(\delta_{\sigma,\pm\pi/2} - \delta_{\sigma,0} - \delta_{\sigma,\pi}) + E(\Psi^N_{-N})$	$\Psi(S) = \Psi^{s+}_{s-}$
D	$\epsilon(\Psi_R) + 2\Delta S + ([2N]/2)[1 + \delta_{0q}(\delta_{\sigma,\pm\pi/2} - \delta_{\sigma,0} - \delta_{\sigma,\pi})]\tan\alpha$	$\Psi(D) = \Psi_R \sin\alpha + \Psi^{s+,s+}_{s-,s-} \cos\alpha$
	C Perturbation ($c^- > 0$, $s^+ = 0$)	
N_α	$E(\Psi^{l-}_{s-}) - c^- \tan\beta$	$\Psi(N_\alpha) = \Psi^{l-}_{s-} \cos\beta + \Psi^{s+}_{h+} \sin\beta$
N_β	$E(\Psi^{l+}_{s-}) - c^- \tan\gamma$	$\Psi(N_\beta) = \Psi^{l+}_{s-} \cos\gamma + \Psi^{s+}_{h-} \sin\gamma$
P_α	$E(\Psi^{l-}_{s-}) + c^-/\tan\beta$	$\Psi(P_\alpha) = \Psi^{l-}_{s-} \sin\beta - \Psi^{s+}_{h+} \cos\beta$
P_β	$E(\Psi^{l+}_{s-}) + c^-/\tan\gamma$	$\Psi(P_\beta) = \Psi^{l+}_{s-} \sin\gamma - \Psi^{s+}_{h-} \cos\gamma$
	S Perturbation ($s^+ > 0$, $c^- = 0$)	
N_α	$E(\Psi^{l+}_{s-}) - s^+ \tan\beta'$	$\Psi(N_\alpha) = \Psi^{l+}_{s-} \cos\beta' + \Psi^{s+}_{h+} \sin\beta'$
N_β	$E(\Psi^{l-}_{s-}) - s^+ \tan\gamma'$	$\Psi(N_\beta) = \Psi^{l-}_{s-} \cos\gamma' - \Psi^{s+}_{h-} \sin\gamma'$
P_α	$E(\Psi^{l+}_{s-}) + s^+/\tan\beta'$	$\Psi(P_\alpha) = \Psi^{l+}_{s-} \sin\beta' - \Psi^{s+}_{h+} \cos\beta'$
P_β	$E(\Psi^{l-}_{s-}) + s^+/\tan\gamma'$	$\Psi(P_\beta) = \Psi^{l-}_{s-} \sin\gamma' + \Psi^{s+}_{h-} \cos\gamma'$

[a] $\epsilon(\Psi_R) = E(\Psi^N_{-N}) - \Delta S + ([2N]/2)[(1 - \delta_{0q}(\delta_{\sigma,\pi/2} - \delta_{\sigma,0})]$; $\alpha = (^1/_2)\tan^{-1}\{[2N][1 + \delta_{0q}(\delta_{\sigma,\pi/2} - \delta_{\sigma,0})]/2\Delta S\}$; $\delta_{\sigma,\omega}$ equals 1 if $\sigma = \omega$, and 0 otherwise; see eq 20 for definitions of configuration energies, eq 27 for β, eq 28 for γ, eq 29 for β', eq 30 for γ', and eq 18 for c^-, s^+, and $\rho^\pm$.

spectrum, and for the dipole strength D, which characterizes absorption intensities.

For low-symmetry molecules devoid of degenerate states, the contribution to the MCD spectrum due to the transition from the ground-state G into the excited state F is given by

$$[\Theta]_M = -21.3458 f_2 B(G \rightarrow F) \tag{22}$$

where $[\Theta]_M$ is the magnetically induced molar ellipticity per unit magnetic field in deg L m^{-1} mol^{-1} G^{-1}, the line shape function f_2 is that of an absorption line, and $B(G \rightarrow F)$ is the B term of the G $\rightarrow$ F transition in units of D^2 β_e/cm^{-1}. A negative (positive) B term corresponds to a positive (negative) peak in the MCD spectrum.

The values of the B terms are usually obtained from the measured isotropic solution spectra by the method of moments

$$B = -33.53^{-1} \int d\tilde{\nu} [\Theta]_M / \tilde{\nu} \tag{23}$$

where $\tilde{\nu}$ is the wavenumber. The integration is over the region of the G $\rightarrow$ F transition.

If one ignores vibrational fine structure, the following expression for B in molecules without degenerate states results from the use of first-order perturbation theory for the effect of the magnetic field[14]

$$B(G \rightarrow F) = \sum_{K,K \neq F} B^F_{K,F} + \sum_{K,K \neq G} B^F_{K,G}$$

$$B^F_{K,F} = \mathrm{Im}\{[\langle F|\hat{M}|K\rangle \cdot \langle G|\hat{\boldsymbol{M}}|F\rangle \times \langle K|\hat{\boldsymbol{M}}|G\rangle]\Delta^{-1}(K,F)\}$$

$$B^F_{K,G} = \mathrm{Im}\{[\langle K|\hat{M}|G\rangle \cdot \langle G|\hat{\boldsymbol{M}}|F\rangle \times \langle F|\hat{\boldsymbol{M}}|K\rangle]\Delta^{-1}(K,G)\}$$

$$\Delta^{-1}(X,Y) \equiv [E(X) - E(Y)]^{-1} \tag{24}$$

where E(I) denotes the energy of the state I, the summation over K runs over all electronic states except as shown, the wave functions $|G\rangle$, $|K\rangle$, and $|F\rangle$ are those in the absence of magnetic field, and Im stands for "imaginary part of".

The dipole strength D is defined by

$$D(G \rightarrow F) = |\langle F|\hat{\boldsymbol{M}}|G\rangle|^2 \tag{25}$$

The 3 × 3 Matrix. Properties of the Ground and the Intrashell Excited Electronic States. These results are the same as for high-symmetry molecules (part 2[1]); they will be summarized only briefly. Diagonalization of the 3 × 3 matrix 16 (cf. eq 20) yields the ground (G) and two excited (S, D) states of the perturbed parent 4*N*-electron [*n*]annulene perimeter. Their wave functions and energies are given in Table 1. The S and D states have no analogues in molecules derived from aromatic perimeters, in which intrashell excitation is not possible.

The ground state wave function depends on the value of the phase angle σ and the magnitude $\Delta S/2$ of the SO level perturbation (for more detail, see ref 13). If the perimeter is charged ($4N \neq n$), explicit expressions for the eigenvalues and eigenfunctions of the 3 × 3 matrix are obtained easily. For uncharged perimeters, the problem is diagonal or block diagonal when $\sigma = I\pi/2$, where I is an integer, and the algebraic solution is then simple. This is guaranteed if at least one symmetry plane perpendicular to the molecular plane is present, and this will be assumed presently. The general case requires a diagonalization of the full 3 × 3 matrix, and the wave functions cannot be written very simply in closed form.

(i) Uncharged Perimeters. For $\sigma = 0$ or π (heterosymmetric biradicaloids; if a symmetry plane is present, as we shall assume in this paper, it passes through atom 0), the 3 × 3 matrix is diagonal and either Ψ^{s+}_{s-} or Ψ_R could represent the ground state in principle, depending on the magnitude of ΔS. Now we only consider molecules with $\Delta S > 2[2N]$, and Ψ_R is the ground-state wave function. For $\sigma = \pm\pi/2$ (homosymmetric biradicaloids; if a symmetry plane is present, it passes through two bond midpoints), Ψ_R and $\Psi^{s+,s+}_{s-,s-}$ interact through the two-electron integral $[2N]$ and the magnitude of ΔS determines the relative contributions of the two configurations to the ground state. With increasing ΔS, the weight of Ψ_R in the ground state increases rapidly. The wave function of the ground state G is

$$\Psi(G) = \Psi_R \cos\alpha - \Psi^{s+,s+}_{s-,s-} \sin\alpha \tag{26}$$

with $\alpha = (^1/_2)\tan^{-1}([2N]/\Delta S)$, $0 \leq \alpha \leq \pi/4$. For $\Delta S = 2[2N]$, $\alpha = 13°$, and the weight of Ψ_R in the ground state is 95%. For larger values of ΔS, this weight is even higher.

Even in the general case (nonsymmetrical biradicaloid; σ not equal to an integral multiple of $\pi/2$), when the 3 × 3 matrix is not block diagonal, the ground state wave function is again well approximated by Ψ_R when ΔS is sufficiently large.

(ii) Charged Perimeters. The ground-state wave function for any perturbed charged 4*N*-electron system with $\Delta S \neq 0$ is given by eq 26, where α now equals $(^1/_2)\tan^{-1}([2N]/2\Delta S)$. For $\Delta S = 2[2N]$, $\alpha = 7°$ and the weight of Ψ_R in the ground state is 98.5%.

The identification of $\Psi(G)$ with Ψ_R characterizes an unaromatic (or ambiaromatic) as opposed to an antiaromatic species and permits the use of a 7-dimensional basis set as opposed to the 11-dimensional basis set of part 1.[8] This identification is certainly sensible for both uncharged and charged perimeters if the perturbation is strong enough to cause ΔS to exceed $2[2N]$. In the following development of formulas for spectroscopic observables for unaromatic (or ambiaromatic) π systems from the perimeter model, we therefore use $\Psi(G) = \Psi_R$, i.e., $\alpha = 0$, unless specified otherwise. If one wished to retain the effect of nonvanishing α, a multiplicative factor of $\cos^2 \alpha$ would have to be added to all expressions for B and D terms and a multiplicative term $(1 + \tan \alpha)$ would have to be added to the $B^F_{S,G}$ contributions to B terms. The resulting changes are negligible relative to the uncertainties of the present simple model.

(iii) Summary of Spectral Properties. The proposed state labels, S at lower energy and D at higher energy, reflect the fact that for a large ΔS the former is predominantly singly (HOMO $\rightarrow$ LUMO) and the latter doubly (HOMO$^2 \rightarrow$ LUMO^2) excited relative to the G state. Since the electric dipole transition moments from G to S and D are zero in the present model, one expects the two transitions to be weak in absorption and MCD spectra, and no predictions of MCD signs are possible. The G $\rightarrow$ S transition is reminiscent of the $n \rightarrow \pi^*$ transition in formaldehyde in that it is electric dipole forbidden and magnetic dipole allowed. Chiral perturbations are likely to induce natural circular dichroism with a large dissymmetry factor g.

The forbidden transition into the D state appears at considerably higher energies and is very likely to be covered up by other transitions. Indeed, transitions into the D state of unaromatic or ambiaromatic molecules are hardly ever observed, and the inability of the simple model to predict the sign of this MCD term is not a serious deficiency.

The 4 × 4 Matrix. Properties of Intershell Excited Electronic States. Transitions from the ground state into the four states that result from the diagonalization of the 4 × 4 matrix 17 (cf. eq 20) usually dominate the optical spectrum of an unaromatic or ambiaromatic molecule. Superficially, these transitions resemble the L and B transitions of aromatic molecules. The perimeter model provides useful predictions of transition intensity, polarization, and MCD sign, often accessible without recourse to a computer.

In general, a low-symmetry perturbation will lift the degeneracies of all orbital levels (Figure 1), configurations, and states. Overall, we then expect a total of four distinct transitions into intershell excited states in addition to the already discussed transitions into the S and D states. In an obvious extension of the notation used for the high-symmetry systems of part 2,[1] the six excited states that originate in the S, D, N, and P states of the high-symmetry case of part 2[1] will be labeled S, D, N_α, N_β, P_α, and P_β for the moment (a more definitive nomenclature is proposed below). Relative to the high-symmetry case, the loss of state degeneracy causes A terms to vanish but provides additional contributions to the B terms, owing to the mutual magnetic mixing within the N_α, N_β and P_α, P_β state pairs. The dipole strength for the transitions into the N_α, N_β, and P_α, P_β state pairs is distributed between the two members of each pair and therefore remains smaller for both N states than it is for the two P states.

The energy ordering of the configurations is determined by all three parameters, ΔHSL, ΔH, and ΔL, and the phase angles η, σ, and λ may all be different. For general values of these angles the algebraic solution is extremely complicated since all four configurations in matrix 17 mix. Useful solutions are obtained in cases characterized by values of the combination phase angles ρ^+ and ρ^- (eq 18) equal to integer multiples of $\pi/2$. Such values are guaranteed in the presence of at least one plane of mirror reflection perpendicular to the plane of the molecule, assumed presently. This is reminiscent of the previously treated situation for perturbed aromatic perimeters.[3,4,5] When ρ^-, and for uncharged perimeters, also ρ^+, is equal to an integer multiple of $\pi/2$, the 4 × 4 matrix 17 factorizes into two 2 × 2 matrices since either c^- or s^+ vanishes, and simple solutions result (recall that for singly charged perimeters we neglect the 4 × 3 matrix 19).

Since the configurations mix only pairwise, we can reserve the label α for the two equally polarized states (N_α, P_α) that contain the Ψ^{s+}_{h+} configuration and the label β for the states (N_β, P_β) that contain the Ψ^{s+}_{h-} configuration and also have equal transition moment directions. Depending on whether c^- or s^+ vanishes, we need to treat two classes of perturbations: for C perturbations, ρ^+ and ρ^- are even multiples of $\pi/2$, $c^- > 0$ and $s^+ = 0$; for S perturbations, ρ^+ and ρ^- are odd multiples of $\pi/2$, $c^- = 0$ and $s^+ > 0$. The signs of c^- and s^+ are immaterial since they change when 2π is added to η or λ. We take them to be positive.

Molecules with a plane of symmetry perpendicular to the molecular plane are of the C class if the orbitals h_- and l_- have identical symmetry with respect to reflection in the plane; otherwise, they are of the S class. When the symmetry plane passes through an atom and the x, y axes thus are symmetry adapted; inspection of eq 14 shows that the G $\rightarrow N_\alpha$, G $\rightarrow P_\alpha$ transitions are polarized along x and the G $\rightarrow N_\beta$, G $\rightarrow P_\beta$ transitions along y if $\eta = \sigma$ and that the reverse is true if $\eta = \sigma + \pi$ (recall that x passes through the perimeter atom labeled $\mu = 0$). When the symmetry plane passes only through bond midpoints, the x axis passes through the atom located immediately counterclockwise next to the midpoint. In the presence of two such symmetry planes, one of them needs to be chosen for this purpose. Once the choice of a bond midpoint and x axis direction is made, and the phase angles are thus fixed, the α transitions are polarized in the symmetry axis that passes through the midpoint if $\eta = \sigma - 2\pi/n$ and they are polarized perpendicular to this symmetry axis if $\eta = \sigma - 2\pi/n + \pi$. The β transitions are polarized perpendicular to the α transitions.

The most general class of perturbation can only occur in the absence of a plane of symmetry perpendicular to the molecular plane. It contains a C and an S perturbation simultaneously ($c^- \neq 0$, $s^+ \neq 0$, mixed perturbation) and leads to results too complicated to be useful. It will not be considered in the following.

Since the ordering of configuration energies is of crucial importance for the prediction of the spectroscopic observables, Figure 2 shows all possibilities as a function of the magnitudes of the orbital splitting sum ΣHL, the absolute value of the orbital splitting difference $|\Delta HL|$, and the absolute value of the orbital shift difference $|\Delta HSL|$. The "orbital-shift-dominated" case is characterized by $|\Delta HSL| > |\Delta HL|$, the "orbital-splitting-dominated" case, by $\Sigma HL > |\Delta HL| > |\Delta HSL|$, and the more complex intermediate cases, by $\Sigma HL \geq |\Delta HSL| \geq |\Delta HL|$. If $\Sigma HL \simeq |\Delta HSL|$ in an S-perturbed system, and if $|\Delta HSL| \simeq |\Delta HL|$ in a C-perturbed system, this intermediate case is still relatively simple. Figure 2 shows that the value of $|\Delta HSL|$ relative to ΣHL and $|\Delta HL|$ is the primary factor that determines the order of the N_α, N_β, P_α, and P_β states.

The algebraic results are collected in Table 1 (state energies and wave functions) and Tables 2 and 3 (dipole strengths and

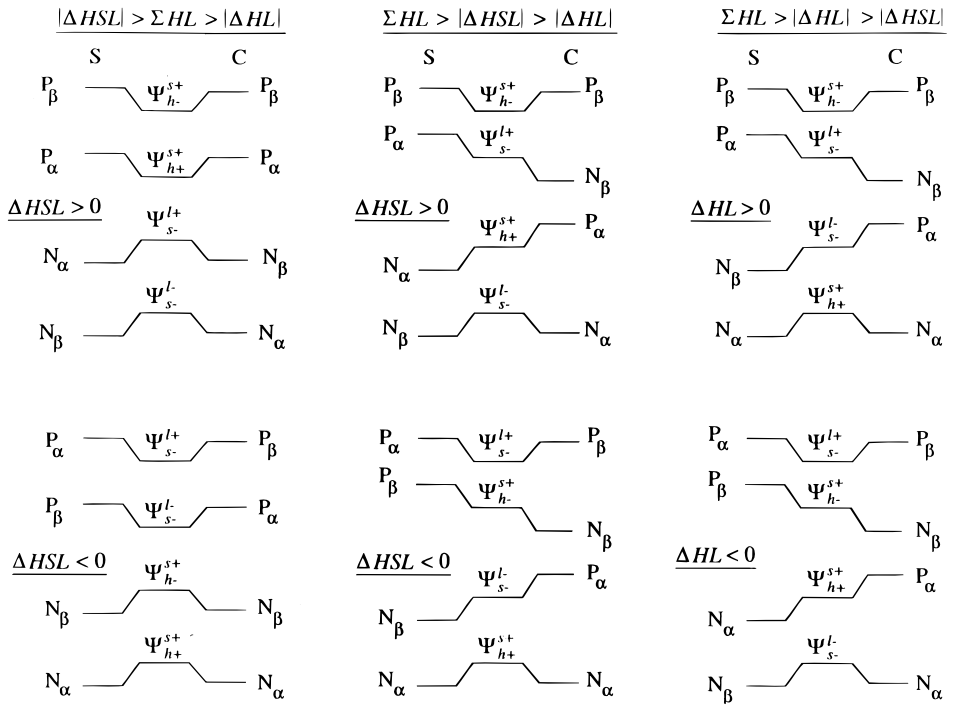

Figure 2. Illustrative relative energies of the four "intershell" excited configurations as a function of ΔHSL, ΔHL, and ΣHL, and the effect of their structural mixing by C and S types of perturbation of a $4N$-electron [n]annulene. Left and center, orbital-shift-dominated cases; right, orbital-splitting-dominated cases.

TABLE 2: Low-Symmetry C-Perturbed ($c^- > 0$, $s^+ = 0$) Unaromatic and Ambiaromatic $4N$-Electron [n]Annulenes ($\Delta S > 2[2N]$, ΔH, $\Delta L \neq 0$): Dipole Strength D and the MCD B Term for Transitions from the Ground State G[a]

state	D	B
S	0	0
D	0	0
N_α	$(m^- \sin\beta - m^+ \cos\beta)^2$	$-\Delta^{-1}(S, G)\mu(n, N)(m^+ \cos\beta - m^- \sin\beta)(m^+ \cos\beta + m^- \sin\beta)$ $-\Delta^{-1}(N_\beta, N_\alpha)(\cos\beta \cos\gamma\, \mu(n, N+1) - \sin\beta \sin\gamma\, \mu(n, N-1))(m^+ \cos\beta - m^- \sin\beta)(m^+ \cos\gamma - m^- \sin\gamma)$ $-\Delta^{-1}(P_\beta, N_\alpha)(\cos\beta \sin\gamma\, \mu(n, N+1) + \sin\beta \cos\gamma\, \mu(n, N-1))(m^+ \cos\beta - m^- \sin\beta)(m^+ \sin\gamma + m^- \cos\gamma)$
N_β	$(m^- \sin\gamma - m^+ \cos\gamma)^2$	$-\Delta^{-1}(S, G)\mu(n, N)(m^+ \cos\gamma - m^- \sin\gamma)(m^+ \cos\gamma + m^- \sin\gamma)$ $-\Delta^{-1}(N_\beta, N_\alpha)(\cos\beta \cos\gamma\, \mu(n, N+1) - \sin\beta \sin\gamma\, \mu(n, N-1))(m^+ \cos\beta - m^- \sin\beta)(m^- \sin\gamma - m^+ \cos\gamma)$ $-\Delta^{-1}(P_\alpha, N_\beta)(\cos\gamma \sin\beta\, \mu(n, N+1) + \sin\gamma \cos\beta\, \mu(n, N-1))(m^+ \cos\gamma - m^- \sin\gamma)(m^+ \sin\beta + m^- \cos\beta)$
P_α	$(m^+ \sin\beta + m^- \cos\beta)^2$	$+\Delta^{-1}(S, G)\mu(n, N)(m^+ \cos\beta - m^- \sin\beta)(m^+ \cos\beta + m^- \sin\beta)$ $+\Delta^{-1}(P_\alpha, N_\beta)(\cos\gamma \sin\beta\, \mu(n, N+1) + \sin\gamma \cos\beta\, \mu(n, N-1))(m^+ \cos\gamma - m^- \sin\gamma)(m^+ \sin\beta + m^- \cos\beta)$ $-\Delta^{-1}(P_\beta, P_\alpha)(\sin\beta \sin\gamma\, \mu(n, N+1) - \cos\beta \cos\gamma\, \mu(n, N-1))(m^+ \sin\beta + m^- \cos\beta)(m^+ \sin\gamma + m^- \cos\gamma)$
P_β	$(m^+ \sin\gamma + m^- \cos\gamma)^2$	$+\Delta^{-1}(S, G)\mu(n, N)(m^+ \cos\gamma - m^- \sin\gamma)(m^+ \cos\gamma + m^- \sin\gamma)$ $+\Delta^{-1}(P_\beta, N_\alpha)(\cos\beta \sin\gamma\, \mu(n, N+1) + \sin\beta \cos\gamma\, \mu(n, N-1))(m^+ \cos\beta - m^- \sin\beta)(m^+ \sin\gamma + m^- \cos\gamma)$ $+\Delta^{-1}(P_\beta, P_\alpha)(\sin\beta \sin\gamma\, \mu(n, N+1) - \cos\beta \cos\gamma\, \mu(n, N-1))(m^+ \sin\beta + m^- \cos\beta)(m^+ \sin\gamma + m^- \cos\gamma)$

[a] Assuming $\Psi(G) = \Psi_R$, i.e., $\alpha = 0$. See eqs 27 and 28 for definitions of β and γ, respectively.

B terms). They describe configuration interaction in terms of the mixing angles β, β', γ, and γ', which are determined by the molecular orbital characteristics $|\Delta HSL|$, $|\Delta HL|$, and ΣHL. When β or β' (γ or γ') is smaller than $\pi/4$, N_α (N_β) is dominated by an SO $\rightarrow$ LO configuration and P_α (P_β) by the HO $\rightarrow$ SO configuration. When β or β' (γ or γ') is larger than $\pi/4$, the opposite is true. The domination of the SO $\rightarrow$ LO configurations or the HO $\rightarrow$ SO configurations in the lower excited states relates physically to the relative ease of excitation of electrons or holes from the half-occupied "Fermi level", and it largely dictates the signs of B terms in MCD spectra. Since sufficient information about the relative values of $|\Delta HSL|$, $|\Delta HL|$, and ΣHL is usually facile to deduce from molecular structure using simple perturbation theory,[9,12] qualitative predictions of B term signs become easy.

Quantitative expressions for each nonvanishing B term in the MCD spectra (Tables 2 and 3) consist of three contributions, $B^F_{S,G}$, $B^F_{N\zeta,F}$, and $B^F_{P\zeta,F}$, where ζ equals either α or β. The $B^F_{S,G}$ contributions are due to the magnetic mixing of the S state into the ground-state G. The signs of these contributions to the B term of the F-th transition only depend on the relative magnitudes of the coefficients of the SO $\rightarrow$ LO and HO $\rightarrow$ SO configurations and are plus for the two states dominated by the SO $\rightarrow$ LO configurations and minus for the two states dominated by the HO $\rightarrow$ SO configurations. However, the magnitude of these contributions is greatly reduced by the relatively large energy difference denominator caused by the large energy difference between the G and S states, and the $B^F_{S,G}$ contributions rarely, if ever, dominate the B terms.

The more important contributions $B^F_{N\zeta,F}$ and $B^F_{P\zeta,F}$ to the B term of the F-th transition that are due to the mutual magnetic mixing of the excited states N_ζ and P_ζ with F, respectively, are superimposed on the $B^F_{S,G}$ contribution. They generally benefit from much smaller magnitudes of the energy denominators and normally determine the resulting B term signs.

C-Perturbed Perimeters (Tables 1 and 2). In this most commonly encountered case, N_α always lies below N_β and P_α below P_β. State energies increase in the order N, N, P, P in the orbital-shift-dominated case, in which the N state pair is very

TABLE 3: Low-Symmetry S-Perturbed ($c^- = 0$, $s^+ > 0$) Unaromatic and Ambiaromatic 4*N*-Electron [*n*]Annulenes ($\Delta S > 2[2N]$, $\Delta H,\Delta L \neq 0$): Dipole Strength *D* and the MCD *B* Term for Transitions from the Ground State G[a]

state	*D*	*B*
S	0	0
D	0	0
N_α	$(m^- \sin\beta' - m^+ \cos\beta')^2$	$-\Delta^{-1}(S, G)\mu(n, N)(m^+ \cos\beta' - m^- \sin\beta')(m^+ \cos\beta' + m^- \sin\beta')$ $+\Delta^{-1}(N_\alpha, N_\beta)[\cos\gamma' \cos\beta'\mu(n, N+1) - \sin\gamma' \sin\beta'\mu(n, N-1)](m^+ \cos\gamma' - m^- \sin\gamma')(m^+ \cos\beta' - m^- \sin\beta')$ $-\Delta^{-1}(P_\beta, N_\alpha)[\sin\gamma' \cos\beta'\mu(n, N+1) + \cos\gamma' \sin\beta'\mu(n, N-1)](m^+ \cos\beta' - m^- \sin\beta')(m^+ \sin\gamma' + m^- \cos\gamma')$
N_β	$(m^+ \cos\gamma' - m^- \sin\gamma')^2$	$-\Delta^{-1}(S, G)\mu(n, N)(m^+ \cos\gamma' - m^- \sin\gamma')(m^+ \cos\gamma' + m^- \sin\gamma')$ $-\Delta^{-1}(N_\alpha, N_\beta)[\cos\gamma' \cos\beta'\mu(n, N+1) - \sin\gamma' \sin\beta'\mu(n, N-1)](m^+ \cos\gamma' - m^- \sin\gamma')(m^+ \cos\beta' - m^- \sin\beta')$ $-\Delta^{-1}(P_\alpha, N_\beta)[\cos\gamma' \sin\beta'\mu(n, N+1) + \sin\gamma' \cos\beta'\mu(n, N-1)](m^+ \cos\gamma' - m^- \sin\gamma')(m^+ \sin\beta' + m^- \cos\beta')$
P_α	$(m^+ \sin\beta' + m^- \cos\beta')^2$	$+\Delta^{-1}(S, G)\mu(n, N)(m^+ \cos\beta' - m^- \sin\beta')(m^- \sin\beta' + m^+ \cos\beta')$ $+\Delta^{-1}(P_\alpha, N_\beta)[\cos\gamma' \sin\beta'\mu(n, N+1) + \sin\gamma' \cos\beta'\mu(n, N-1)](m^+ \cos\gamma' - m^- \sin\gamma')(m^+ \sin\beta' + m^- \cos\beta')$ $+\Delta^{-1}(P_\alpha, P_\beta)[\sin\gamma' \sin\beta'\mu(n, N+1) - \cos\gamma' \cos\beta'\mu(n, N-1))(m^+ \sin\gamma' + m^- \cos\gamma')(m^+ \sin\beta' + m^- \cos\beta')$
P_β	$(m^- \cos\gamma' + m^+ \sin\gamma')^2$	$+\Delta^{-1}(S, G)\mu(n, N)(m^+ \cos\gamma' - m^- \sin\gamma')(m^+ \cos\gamma' + m^- \sin\gamma')$ $+\Delta^{-1}(P_\beta, N_\alpha)(\sin\gamma' \cos\beta'\mu(n, N+1) + \cos\gamma' \sin\beta'\mu(n, N-1))(m^+ \cos\beta' - m^- \sin\beta')(m^+ \sin\gamma' + m^- \cos\gamma')$ $-\Delta^{-1}(P_\alpha, P_\beta)[\sin\gamma' \sin\beta'\mu(n, N+1) - \cos\gamma' \cos\beta'\mu(n, N-1)](m^+ \sin\gamma' + m^- \cos\gamma')(m^+ \sin\beta' + m^- \cos\beta')$

[a] Assuming $\Psi(G) = \Psi_R$, i.e., $\alpha = 0$. See eqs 29 and 30 for definitions of β' and γ', respectively.

well separated from the P state pair and the mutual magnetic mixing within each of these two pairs of states dominates their MCD *B* terms. In the other cases, the order N, P, N, P is possible. In the orbital-splitting-dominated case, magnetic mixing within the N and P state pairs only dominates the *B* terms of the lowest ($G \rightarrow N_\alpha$) and the highest ($G \rightarrow P_\beta$) of the four transitions. The *B* terms of the two middle transitions ($G \rightarrow N_\beta$, $G \rightarrow P_\alpha$) are determined by the mutual magnetic mixing of their excited states.

The signs of the contributions to *B* terms are determined by the values of β and γ, defined by

$$\beta = (^1/_2)\tan^{-1}(2\langle\Psi_{s-}^{l-}|\hat{H}|\Psi_{h+}^{s+}\rangle/[E(\Psi_{s-}^{l-}) - E(\Psi_{h+}^{s+})]) = (^1/_2)\tan^{-1}[4c^-/(\Delta HSL - \Delta HL + Y)] \quad (27)$$

$$Y = [2N-1] - [2N+1] + \delta_{-2q}([2N] + [2N-1]) \times \cos(\eta + \sigma) - \delta_{+2q}([2N] + [2N+1])\cos(\lambda + \sigma)$$

$$\gamma = (^1/_2)\tan^{-1}(2\langle\Psi_{s-}^{l+}|\hat{H}|\Psi_{h-}^{s+}\rangle/[E(\Psi_{s-}^{l+}) - E(\Psi_{h-}^{s+})]) = (^1/_2)\tan^{-1}[4c^-/(\Delta HSL + \Delta HL + Z)] \quad (28)$$

$$Z = [2N-1] - [2N+1] - \delta_{-2q}([2N] + [2N-1]) \times \cos(\eta + \sigma) + \delta_{+2q}([2N] + [2N+1])\cos(\lambda + \sigma)$$

The two factors that dominate the magnitudes of β and γ are the orbital energy combinations ΔHSL and ΔHL, since the terms *Y* and *Z* are small. Both $[2N-1]$ and $[2N+1]$ are small and nearly equal, and their difference will typically be negligible. Also, the remaining terms in *Y* and *Z* only contain small electron repulsion integrals; moreover, they are only present if the parent perimeter is doubly charged. In the following discussion, *Y* and *Z* will therefore be considered negligible (a small nonzero value of *Y* means that β will reach $\pi/4$ when $\Delta HSL - \Delta HL = -Y \simeq 0$ instead of $\Delta HSL - \Delta HL = 0$).

(i) Orbital-Shift-Dominated Systems, $|\Delta HSL| > |\Delta HL|$ (center top and bottom in Figure 3). These are of two kinds, which differ in state order and correspond to the left and center columns in Figure 2.

In the first case, the orbital splittings themselves are not very large, and $|\Delta HSL| > \Sigma HL > |\Delta HL|$. In this instance, the members of the low-energy N_α, N_β pair are close in energy and so are the members of the high-energy P_α, P_β pair (left column in Figure 2). Magnetic mixing within these pairs prevails, and the $B^F_{N\beta,N\alpha}$ and $B^F_{P\beta,P\alpha}$ terms are dominant. The

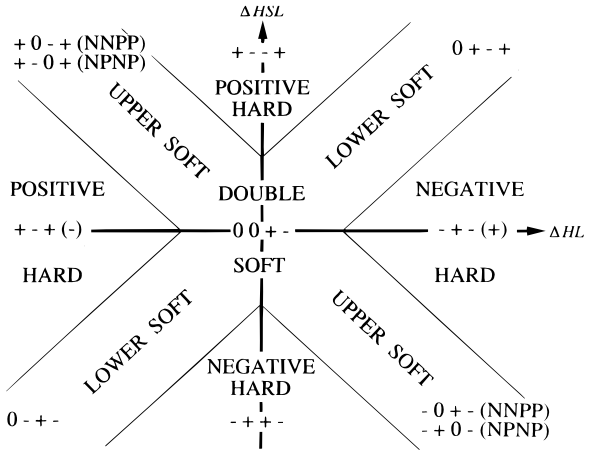

Figure 3. Anticipated *B* term sign pattern for the N and P states of a C-perturbed 4*N*-electron [*n*]annulene perimeter in the order of increasing energy, as a function of ΔHSL and ΔHL, assuming $|\Delta HSL| > \Sigma HL$ for hard chromophores (if $|\Delta HSL| < \Sigma HL$, the sign sequence changes to $++-+$ for positive hard and $--+-$ for negative hard ones). If the state energy order is N, N, P, P, $+0-+$ applies when $\Delta HSL \simeq -\Delta HL > 0$ and $-0+-$ applies when $\Delta HSL \simeq -\Delta HL < 0$. If the state order is N, P, N, P, $+-0+$ applies when $\Delta HSL \simeq -\Delta HL > 0$ and $-+0-$ applies when $\Delta HSL \simeq -\Delta HL < 0$. At the $\Delta HSL = \Delta HL = 0$ point, the four *B* terms collapse into two *A* terms if $\Sigma HL = 0$, but the sign sequence remains (cf. part 2[1]).

sign of the denominator in the expressions 27 and 28 for β and γ is dictated by the sign of ΔHSL. A positive value implies $0 \leq \beta,\gamma < \pi/4$. The *B* terms of the N_α and N_β states are dominated by the $B^F_{N\beta,N\alpha}$ contribution, and this yields a positive *B* term for the lower and a negative *B* term for the higher of the two $G \rightarrow N$ transitions. The $B^F_{S,G}$ contributions to both terms are positive, supporting the sign for the lower transition, but decreasing the magnitude of the B term for the upper transition with only a very slight chance of reversing it, because $\Delta^{-1}_{N\beta,N\alpha}$ is expected to be significantly larger than $\Delta^{-1}_{S,G}$.

The MCD terms for the transitions to the P_α and P_β states are dominated by $B^F_{P\beta,P\alpha}$, and one expects a negative *B* term for the transition to the lower and a positive *B* term for that to the higher lying P state. Again the $B^F_{S,G}$ terms support the sign for the lower $G \rightarrow P_\alpha$ transition and oppose the $B^{P\beta}_{P\alpha,P\beta}$ contribution to the higher one. Here, the $B^{P\beta}_{S,G}$ term may change the sign for the latter transition because the separation of the P_α and P_β states may be increased by additional interactions with other excited states, but the higher of the two P states is expected to occur at such high energies that this transition will hardly ever be observed below 50 000 cm^{-1}. In general, we expect a $+-\ -+$

MCD *B* term sign pattern in the order of increasing energy for the four N and P states.

A negative value of ΔHSL implies $\pi/4 < \beta, \gamma \leq \pi/2$. This change in the values of β and γ changes the sign of every MCD *B* term contribution in Table 2 and will therefore change the signs of all MCD terms relative to the above case of positive ΔHSL. Thus, the *B* term sign pattern $-++-$ is expected for the four transitions in these systems instead of the $+--+$ pattern derived above for $\Delta HSL > 0$.

In the second case, the orbital splittings are large but approximately equal, and $\Sigma HL > |\Delta HSL| > |\Delta HL|$. In this instance, the upper N state, N_β, is close in energy to the lower P state, P_α (central column in Figure 2). Either order, N_β below or above P_α, is possible (the latter order is shown in Figure 2). Magnetic mixing of these two states prevails, and the $B^{F}_{N\beta,P\alpha}$ term is dominant. The sign of the denominator in the expressions 27 and 28 for β and γ is again dictated by the sign of ΔHSL. A positive value implies $0 \leq \beta,\gamma < \pi/4$, providing the lower of the two states with a positive *B* term and the upper one with a negative *B* term. The *B* term of the N_α state is dominated by the $B^{N\alpha}_{N\beta,N\alpha}$ contribution, and this yields a positive *B* term for the lower energy $G \rightarrow N_\alpha$ transition. The $B^{F}_{S,G}$ contributions to the *B* terms of both $G \rightarrow N$ transitions are positive, supporting the sign for the lower transition, and also for the upper transition if N_β lies below P_α, but decreasing the magnitude of the B term for the transition into the N_β state if it lies above P_α, with only a very slight chance of reversing it, because $\Delta^{-1}_{N\beta,P\alpha}$ is expected to be significantly larger than $\Delta^{-1}_{S,G}$.

The MCD term for the transitions to the P_α state is opposite to that of the N_β state, since both are dominated by $B^{F}_{N\beta,P\alpha}$, and one expects a positive *B* term if P_α lies below N_β. The *B* term of the higher lying P_β state should be determined by its magnetic mixing with the P_α state and have a positive sign, mostly because its magnetic mixing with N_α suffers from a larger energy difference. The $B^{F}_{S,G}$ terms are negative for transitions into both P states and thus oppose the $B^{P\beta}_{P\alpha,P\beta}$ contribution to $G \rightarrow P_\beta$. They also oppose the $B^{P\alpha}_{N\beta,P\alpha}$ contribution to $G \rightarrow P_\alpha$ if this transition lies below $G \rightarrow N_\alpha$, and support it otherwise. The P_β state is expected to occur at such high energies that it will hardly ever be observed below 50 000 cm^{-1}. Its magnetic mixing with states not included in the model may be important, making the prediction for it less reliable. In general, we expect a $++-+$ MCD *B* term sign pattern in the order of increasing energy for the four N and P states, regardless of the order of the N_β and P_α states.

A negative value of ΔHSL implies $\pi/4 < \beta, \gamma \leq \pi/2$. This change in the values of β and γ changes the sign of every MCD *B* term contribution in Table 2 and will therefore change the signs of all MCD terms relative to the above case of positive ΔHSL. Thus, the *B* term sign pattern $--+-$ is expected for the four transitions in these systems instead of the $++-+$ pattern derived above for $\Delta HSL > 0$.

(ii) Orbital-Splitting-Dominated Systems, $|\Delta HSL| < |\Delta HL|$ (center right and left in Figure 3). In this case, the higher of the N states (N_β) and the lower of the P states (P_α) are close in energy and their mutual magnetic mixing is important. The sign of the denominator in the expressions 27 and 28 for β and γ is dictated by ΔHL, i.e., by the relative size of the splitting of the HO and LO orbitals.

A negative value of ΔHL implies $0 < \beta < \pi/4$ and $\pi/4 < \gamma < \pi/2$. According to Table 2, the signs of the *B* terms for the upper $G \rightarrow N$ transition, $G \rightarrow N_\beta$, and the lower $G \rightarrow P$ transition, $G \rightarrow P_\alpha$, are dominated by their mutual magnetic mixing, with a negative sign for the lower of the two states and a positive for the upper one. The $B^{F}_{S,G}$ contributions to the four transitions have the signs $+- -+$ in ascending order.

General statements about the $B^{F}_{I,F}$ terms for the lower of the $G \rightarrow N$ transition, $G \rightarrow N_\alpha$, and the higher $G \rightarrow P$ transition, $G \rightarrow P_\beta$, are more difficult to make because the magnetic dipole matrix elements connecting N_α to N_β and P_α to P_β have a smaller magnitude than those connecting N_α to P_β, whereas the magnitude of the energy term $\Delta^{-1}_{I,F}$ is smaller for the latter. Since the $B^{N\alpha}_{S,G}$ and $B^{N\alpha}_{P\beta,N\alpha}$ contributions have the same sign, one would expect a positive *B* term for the lower of the two $G \rightarrow N$ transitions. In contrast, the $B^{P\beta}_{S,G}$ and $B^{P\beta}_{N\alpha,P\beta}$ contributions have opposite signs and although the former is probably smaller, a general prediction of the resulting sign of the *B* term of the high-energy $G \rightarrow P_\beta$ transition is less reliable. Thus, the expected sign pattern is $+-+(-)$ and it is independent of the relative ordering of the higher N state, N_β, and the lower P state, P_α.

For $\Delta HL > 0$ the signs of all *B* term contributions are changed and the expected *B* term sign pattern for the two N states and two P states is $-+-(+)$ in the order of increasing energy.

(iii) Intermediate Systems, $|\Delta HSL| \simeq |\Delta HL| > 0$ (the four corners in Figure 3). In these systems orbital shifting and orbital splitting play a comparable role. Four situations need to be distinguished. If ΔHSL and ΔHL have equal signs, $\beta \simeq \pi/4$. If they are both positive (*pp*), $\gamma \simeq 0$ and if they are both negative (*nn*), $\gamma \simeq \pi/2$. If ΔHSL and ΔHL have opposite signs, $\gamma \simeq \pi/4$. If ΔHSL is positive (*pn*), $\beta \simeq 0$, and if it is negative (*np*), $\beta \simeq \pi/2$.

The sign patterns of the $B^{F}_{S,G}$ contributions are $0+0-$ (*pp*), $0-0+$ (*nn*), $+0-0$ (*pn*), and $-0+0$ (*np*) in the order N_α, N_β, P_α, P_β, where 0 stands for a very small contribution (Table 2). The $B^{F}_{I,F}$ contributions also follow a simple pattern. The mutual magnetic mixing of N_α and N_β makes a negligible contribution in all four cases. This is also true of the $N_\alpha-P_\beta$ mixing in the *pp* and *nn* cases, and of $N_\beta-P_\alpha$ mixing in the *pn* and *np* cases. In the *pp* and *nn* cases, the largest contributions to the *B* terms of the $G \rightarrow N_\beta$ and $G \rightarrow P_\alpha$ transitions originate in the magnetic mixing of the N_β and P_α states. For the lower of the two, the contribution is positive in the *pp* case and negative in the *nn* case. For the upper state, the signs are the opposite. Magnetic mixing of P_α and P_β results in a negative contribution to the *B* term of P_α and a positive one to the *B* term of P_β in the *pp* and *pn* cases, and the signs of the contributions are reversed in the *nn* and *np* cases. In summary, then, for the *pp* case one expects the $0+-+$ sign pattern and for the *nn* case the $0-+-$ pattern in the order of increasing energy. In the *pn* and *np* cases, the magnetic mixing is between N_α and P_β, hampered by their large energy separation, and between the P_α and P_β states. For *pn*, the $N_\alpha-P_\beta$ mixing provides a positive contribution to the *B* term of N_α and a negative one to the *B* term of P_β, and for *np*, it provides the opposite signs. Thus, for the *pn* case, one obtains the $+0-+$ signs for the N_α, N_β, and P_α states, respectively. For the *np* case, the signs are $-0+-$. Figure 3 summarizes the predicted *B* term sign patterns for various choices of ΔHSL and ΔHL. Note that in the *pn* and *np* cases the pattern depends on the state order.

S-Perturbed Perimeters (Tables 1 and 3). In this case, the state order is always N, N, P, P and the order of the α and β states is much less regular than in C-perturbed perimeters, since it is sensitive to the signs and magnitudes of ΔHSL and ΔHL (Figure 2). The signs of the contributions to *B* terms (Table 3)

are determined by the two configuration mixing angles β' and γ'

$$\beta' = (^1/_2)\tan^{-1}[2\langle\Psi_{s-}^{l+}|\hat{H}|\Psi_{h+}^{s+}\rangle/[E(\Psi_{s-}^{l+}) - E(\Psi_{h+}^{s+})] \quad (29)$$
$$= (^1/_2)\tan^{-1}[4s^+/(\Delta HSL - \Sigma HL + Y')]$$

$$Y' = [2N-1] - [2N+1] + \delta_{-2q}([2N] + [2N-1]) \times \cos(\eta + \sigma) + \delta_{+2q}([2N] + [2N+1])\cos(\lambda + \sigma)$$

$$\gamma' = (^1/_2)\tan^{-1}[-2\langle\Psi_{s-}^{l-}|\hat{H}|\Psi_{h-}^{s+}\rangle/[E(\Psi_{s-}^{l-}) - E(\Psi_{h-}^{s+})] \quad (30)$$
$$= (^1/_2)\tan^{-1}[4s^+/(\Delta HSL + \Sigma HL + Z')]$$

$$Z' = [2N-1] - [2N+1] - \delta_{-2q}([2N] + [2N-1]) \times \cos(\eta + \sigma) - \delta_{+2q}([2N] + [2N+1])\cos(\lambda + \sigma)$$

and as in eq 27 and 28, in the following Y' and Z' will be neglected.

(i) Orbital-Shift-Dominated Systems, $|\Delta HSL| > \Sigma HL > |\Delta HL|$ (center top and bottom in Figure 4). The sign of the denominator in eqs 29 and 30 is dictated by the sign of ΔHSL.

If ΔHSL is positive, we have $0 < \beta', \gamma' < \pi/4$. The relative ordering of the states is N_β, N_α, P_α, P_β, with the N state pair well separated from the P state pair, and the mutual magnetic mixing within each pair dominates the B terms: $B^{N\beta}_{N\alpha,N\beta} = -B^{N\alpha}_{N\beta,N\alpha} > 0$ and $B^{P\beta}_{P\alpha,P\beta} = -B^{P\alpha}_{P\beta,P\alpha} > 0$. The $B^F_{S,G}$ contributions are positive for N_β and P_α and negative for N_α and P_β. They reinforce the above result for the N states and work against it for the P states with little chance of reversing it, because of an unfavorable energy denominator. The terms due to N, P mixing are smaller. Thus, one expects the $+-\,-+$ pattern for the four states in the order of increasing energy.

If ΔHSL is negative, we have $\pi/4 < \beta', \gamma' < \pi/2$, and the state order is N_α, N_β, P_β, P_α. This leads to the exactly opposite sign sequence for the B terms, $-++-$.

(ii) Orbital-Splitting-Dominated Systems, $\Sigma HL > |\Delta HSL|$ (center right and left in Figure 4). Now, the sign of the denominator in eqs 29 and 30 is dictated by the positive sign of ΣHL, and as a result, $\pi/4 < \beta' < \pi/2$ and $0 < \gamma' < \pi/4$. The relative ordering of the states is N_α, N_β, P_α, P_β if ΔHL is positive, and N_β, N_α, P_β, P_α if ΔHL is negative. Contributions from magnetic mixing within the N and P state pairs are small despite their small energy separation, and the B terms are likely to be dominated by contributions from N, P mixing: $B^{N\alpha}_{P\beta,N\alpha} = -B^{P\beta}_{N\alpha,P\beta} < 0$ and $B^{N\beta}_{P\alpha,N\beta} = -B^{P\alpha}_{N\beta,P\alpha} > 0$. The $B^F_{S,G}$ contributions reinforce this result for the N states and oppose it for the P states, but should usually be less important, such that the expected sign pattern is $-+-+$ for $\Delta HL > 0$ and $+-+-$ for $\Delta HL < 0$, where the result for the higher P state is not very reliable.

(iii) Intermediate Systems, $|\Delta HSL| \simeq \Sigma HL$ (the four corners in Figure 4). In this case, the contributions from the magnetic mixing of the N states are small despite their energetic proximity, since one or the other of the mixing angles β' and γ' is close to $\pi/4$, and the transition moment from the ground state to the upper N state is therefore very small.

If ΔHSL is positive, $\beta' \simeq \pi/4$ and $0 < \gamma' < \pi/4$ and the energy of the states increases in the order N_β, N_α, P_α, P_β. Mixing of the lower N state with the lower P state gives a positive contribution to the B term of the former, which is not very large since the energy separation of the N and P states is large. This mixing yields a negative contribution to the B term of the latter, which is strongly reinforced by the mutual magnetic mixing of the P states, which provides a positive contribution to the B term of the upper P state. The $B^F_{S,G}$ contribution reinforces the positive B term of the lower N state and weakens the positive B term of the upper P state. It contributes little to the B terms of the other two states. The resulting sign pattern is $+0-+$.

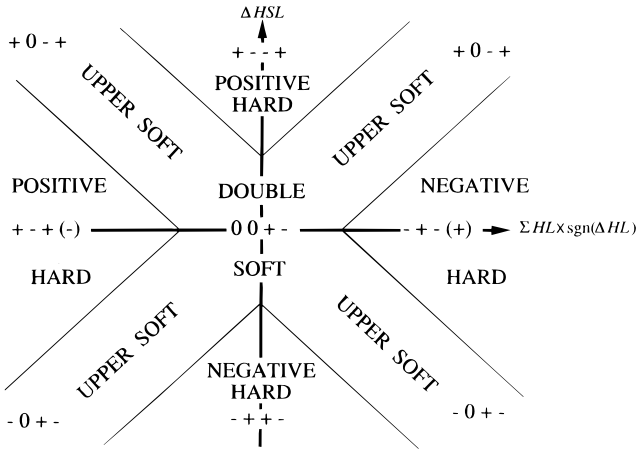

Figure 4. Anticipated B term sign pattern for the N and P states of an S-perturbed 4N-electron [n]annulene perimeter in the order of increasing energy, as a function of ΔHSL and ΣHL(sgnΔHL). At the $\Delta HSL = \Sigma HL = 0$ point, the four B terms collapse into two A terms but the sign sequence remains (cf. part 2[1]).

If ΔHSL is negative, $\pi/4 < \beta' < \pi/2$ and $\gamma' \simeq \pi/4$, the energy order is N_α, N_β, P_β, P_α, and similar arguments predict the exactly opposite sign pattern, $-0+-$. The case of vanishing ΔHSL and vanishing ΣHL has already been treated in part 2;[1] both the N and the P states are degenerate, the transition to the former has no dipole strength and a vanishing B term, and the transition to the latter is intense and has a positive A term.

The expected patterns of B term signs for S-perturbed systems are summarized in Figure 4 as a function of ΔHSL and of ΣHL multiplied by the sign of ΔHL. The sign patterns depend on all three variables, ΣHL (which is always positive), ΔHSL, and ΔHL. However, only the sign of ΔHL and not its magnitude is really important (and that only in the orbital-splitting-dominated case), and the use of ΣHLsgn(ΔHL) in the plot permits us to display in two dimensions results that reflect the effects of all three variables.

Hard and Soft Chromophores

We have shown that in the case of low-symmetry unaromatic and ambiaromatic molecules derived from 4N-electron [n]annulenes that have at least one plane of symmetry perpendicular to the molecular plane, and therefore only two possible mutually perpendicular $\pi\pi^*$ transition directions, one can make predictions of spectral properties from the knowledge of relative orbital energy differences, ΔHSL, ΔHL, and ΣHL (Figure 1). The results thus promise to be as useful as those obtained earlier[3,4,15] for systems derived from $(4N+2)$-electron perimeters.

In all cases, the G → S and G → D transitions are predicted to have no intensity in absorption and in MCD. In practice, the intensities can be expected to be small but nonvanishing and will be probably strongly affected by vibronic effects, which we have ignored presently.

Useful absorption intensity, polarization, and MCD sign predictions are obtained for the four transitions derived from intershell excitation, G → N_α, G → N_β, G → P_α, G → P_β. Transitions into states with equal Greek subscripts have the same polarization direction, while transitions into states with different

Greek subscripts have mutually perpendicular polarization directions. These directions are given by eqs 14: Transitions into α states are polarized along $\boldsymbol{e}_{\eta 1}$ and transitions into β states along $\boldsymbol{e}_{\eta 2}$. While the transitions into the two P states are always intense, the magnitudes and the relative sense of the electric dipole transition moments from the ground to the N states show an interesting structural dependence, which is then reflected in the MCD *B* terms. This dependence originates in the presence of two configurations in the excited-state wave functions, each of which contributes to the transition moment. These contributions have the same sense in the case of the P states, and their sum furnishes these states with large dipole strengths. They have opposite sense in the case of the N states, and their partial or complete cancellation and the resulting sense of the transition moment are dictated by the amplitudes of the two configurations in the excited-state wave function, as described by the appropriate mixing angle, β, γ (eqs 27, 28) or β', γ' (eqs 29, 30). This in turn depends on configuration energies, ultimately dictated by the relative orbital energy differences, ΔHSL, ΔHL, and ΣHL. In the final analysis, these are controlled by the molecular structure, in a way that can be often predicted from qualitative considerations of the PMO type (part 4).[9]

The cancellation of the two contributions to the N state transition moments leads to the most interesting situation, since a slight perturbation of the system may cause the transition moment to increase in one or the other sense, thus changing the sign of the triple vector product in eq 24 that describes the contribution of the magnetic mixing of a state pair toward the MCD *B* term. As the transition moment goes through zero and the contribution changes its sign, the total *B* term is likely to change its sign if this is a dominant contribution, while the oscillator strength, proportional to the square of the transition moment length, drops to zero and increases again. The situation is thus quite analogous to that encountered with perturbed $(4N + 2)$-electron [*n*]annulenes,[3] where we applied the term "soft MCD" chromophore to molecules in which such compensation, or near compensation, occurred. The choice of the label reflects the fact that even a small structural perturbation can alter the sense of the transition moment of one of the L states in such aromatic molecules, and of the N states in the presently considered unaromatic and ambiaromatic ones, and thus change the signs of the *B* terms. Perturbations that totally destroy the cancellation in one or the other sense were said to convert the chromophore into a "hard" one. This choice of label describes the circumstance that once the sense of the transition moment no longer responds to small perturbations, the *B* term signs are stable to minor structural perturbations. In an aromatic chromophore, both L states could be "compensated" ("double-soft" chromophores), or only L_b ("odd-soft" chromophores), or L_a ("even-soft" chromophores).[5]

We propose to use the "soft" and "hard" labels for the unaromatic and ambiaromatic chromophores as well, to facilitate future discussion of the effects of small perturbations on the MCD signs. To proceed, we distinguished (i) C-perturbed perimeters, in which h_-, the lower of the orbitals that resulted from the HOMO of the parent perimeter, and l_-, the lower of the orbitals that resulted from the LUMO of the parent perimeter (eq 6), have the same symmetry [ρ^+ and ρ^- are even multiples of $\pi/2$, eq 18)], and (ii) S-perturbed perimeters, in which h_- and l_- have opposite symmetry (ρ^+ and ρ^- are odd multiples of $\pi/2$).

Soft unaromatic and ambiaromatic chromophores correspond to the "intermediate cases" of the above discussion. In C-perturbed perimeters, the intensity of the transition from the ground state to one of the N states and its *B* term become very small and/or vanish when $|\Delta HSL| \simeq |\Delta HL|$. When ΔHSL and ΔHL have equal signs, this is the lower N state ("lower-soft" chromophore); when they have opposite signs, this is the upper N state ("upper-soft" chromophore). When ΔHSL and ΔHL both vanish, the dipole strengths and the *B* terms of transitions to both N states vanish ("double-soft" chromophore). Alternant hydrocarbons derived from an uncharged perimeter belong to this class as long as the pairing theorem holds at least approximately. If it does not hold very well, e.g., in the presence of four-membered rings, the alternant hydrocarbons will tend to be harder chromophores and ΔHL will determine the sign pattern. When ΣHL vanishes in addition to ΔHSL and ΔHL, the situation reverts to the high-symmetry case discussed in part 2.[1] In S-perturbed perimeters, the intensity of the transition from the ground state to the upper N state and its *B* term become very small or vanish when $|\Delta HSL| \simeq \Sigma HL$. When ΔHSL and ΣHL both vanish, the situation reverts to the high-symmetry case (part 2[1]).

For C-perturbed perimeters, the sign of the quantity $\Delta HSL - \Delta HL$ thus plays a role similar to that played by the sign of $\Delta HOMO - \Delta LUMO$ in the aromatic series.[3,4,15] Since $\Delta HSL - \Delta HL = 2\{[\{E(s_+) + E(s_-)\}/2 - E(h_+)] - [E(l_-) - \{E(s_+) + E(s_-)\}/2]\}$, $\Delta HSL - \Delta HL$ is a measure of the difference of smallest excitation energies of a hole and of an electron from the Fermi level, and it is thus physically reasonable that it should be the key quantity determining the order of MCD signs. For S-perturbed perimeters, the corresponding quantity is $\Delta HSL + \Sigma HL(\mathrm{sgn}\Delta HL)$, which also provides a measure of the relative energies of excitation of a hole and an electron from the Fermi level. For instance, for $\mathrm{sgn}\Delta HL = +1$, one has $\Delta HSL + \Sigma HL = 2\{[\{E(s_+) + E(s_-)\}/2 - E(h_-)] - [E(l_-) - \{E(s_+) + E(s_-)\}/2]\}$.

As in the aromatic series,[3] chromophores in which the approximate equalities that lead to transition moment cancellation are not fulfilled are termed hard. In these chromophores, neither of the transitions into the N states is weak, and neither has a zero *B* term. We classify these chromophores according to the sign of the *B* term of the lower N state. When this is positive, the chromophore is positive-hard, when it is negative, the chromophore is negative-hard.

Summary of MCD Results

The predicted sign patterns are collected in Figures 3 (C perturbation) and 4 (S perturbation), along with the classification of the chromophores into various classes according to the values of ΔHSL, ΔHL, and ΣHL (a simpler version of Figure 3 was derived in our earlier work[6,16] and this is now superseded). We plot ΔHSL vertically in both cases; the horizontal axis is for ΔHL in the case of C-perturbed systems and for $\Sigma HL\mathrm{sgn}(\Delta HL)$ in the case of S-perturbed systems. The sign pattern distribution is identical in both figures, except that for the C-perturbed systems (i) the predictions for the two N states in the case of lower-soft chromophores are interchanged relative to the S-perturbed upper-soft chromophores, and (ii) the order of states is possibly changed from N, N, P, P to N, P, N, P in the case of upper-soft chromophores. In general, a large positive value of ΔHSL and a large negative value of ΔHL or $\Sigma HL(\mathrm{sgn}\Delta HL)$ tend to make a chromophore positive-hard. Since negatively charged perimeters normally have a positive ΔHSL even in the absence of a perturbation, π systems derived from them by weak perturbations will tend to be in this category. Similarly, a large negative value of ΔHSL and a large positive value of ΔHL or $\Sigma HL(\mathrm{sgn}\Delta HL)$ tend to make a chromophore negative-hard. Since

positively charged perimeters normally have a negative ΔHSL even in the absence of a perturbation, π systems derived from them by weak perturbations will tend to be in this category.

Figures 3 and 4 can be used as a quick guide for the prediction of signs of *B* terms of unaromatic MCD chromophores from the knowledge of ΔHSL, ΔHL, and ΣHL. In part 4[9] we discuss in detail some simple procedures that can be used to deduce these quantities from molecular structure, analyze substituent and heteroatom effects, and illustrate the use of the presently deduced rules for *B* term signs in the MCD spectra of acenaphthylene, pleiadiene, their doubly charged ions, and phenalenyl ions. Subsequent papers will deal with the measurement and interpretation of the MCD spectra of several additional families of unaromatic compounds.

Correlation with the States of the Parent Antiaromatic Perimeter

While the correlation of the electronic states of the presently treated low-symmetry unaromatic and ambiaromatic molecules with those of their high-symmetry counterparts examined in part 2[1] is obvious (S → S, D → D, N_α, N_β → N, P_α, P_β → P), the correlation of states of either of these classes with those of the antiaromatic parent perimeter is complicated by the presence of conical intersections in the space spanned by the perturbations. Figure 5 of part 2[1] shows the case of an uncharged perimeter, where the ground state G of a strongly perturbed (unaromatic) perimeter correlates with the lowest singlet state $B_{1g}^{(-)}$ of the parent antiaromatic perimeter along most paths, but correlates with the next higher singlet state $B_{2g}^{(+)}$ of the parent along those paths that go through one of the two conical intersections (cf. Table 3 of part 2[1]). This ambiguity means that the $B_{1g}^{(-)}$ and the $B_{2g}^{(+)}$ states of the parent could equally well be labeled G or S, which is not very useful for nomenclature purposes or for understanding the nature of their wave function. The conical intersections also wreak havoc with attempts to relate the labels of the high-energy N and P states with those of the parent perimeter, and we feel that for uncharged perimeters this is not a productive enterprise. In contrast, the third singlet of the parent, $A_{1g}^{(-)}$, cleanly correlates with the D state of perturbed annulenes. In the ZDO approximation, adopted here, $A_{1g}^{(-)}$ is accidentally degenerate with the second singlet of the parent, $B_{2g}^{(+)}$ (in better approximations it lies a little below it). The D state of the perturbed annulene then correlates with one of the two components of this accidentally degenerate state.

The situation appears more favorable for charged parent perimeters. Here, the degeneracy of the lowest two singlet states occurs in the unperturbed parent perimeter. The G and S states of the unaromatic perturbed perimeters correlate with the two components of the degenerate $E_{2N,g}$ ground state of the antiaromatic parent, and its D state correlates with its next higher A_{1g} state. The lowest two states of the parent could therefore logically be labeled G (or G,S) and D. The correlation of the lower energy more weakly allowed transitions into the N and the higher energy more strongly allowed transitions into the P states of the perturbed perimeter ($\Delta S < 2[2N]$) with transitions in the parent perimeter ($\Delta S = 0$), which generally lie in the opposite order (allowed below forbidden, cf. Figure 3 in ref 8), is unfortunately not straightforward, owing to avoided crossings.

A Proposed General Electronic State Nomenclature for Even-Electron Cyclic π Systems with a Single Perimeter

We are now in a position to propose a general nomenclature for the low-energy states of all systems derived from [*n*]annulene perimeters with an even number of π electrons that have at least one plane of symmetry perpendicular to the molecular plane. The objective is to have excited-state labels that provide as much immediate information about the relative energy, intensity, and polarization direction of transitions from the ground state as possible. These requirements are fulfilled by the original Platt nomenclature developed for aromatic systems derived from uncharged perimeters ($n = 4N + 2$), in that the weaker transitions into the two L states lie below the strong transitions to the two B states, and the polarization direction of transitions into states with subscript a passes through two of the perimeter atoms while the polarization direction of transitions into states with subscript b passes through the midpoints of two of the perimeter bonds. Although either energetic order within the L_a, L_b and B_a, B_b pairs is possible, the transitions are readily identified by their transition moment directions. In molecules of lower symmetry, the L_a, L_b, B_a, and B_b states can mix, but the label of the dominant state can still often be used for state classification purposes.

The L_1, L_2, B_1, B_2 nomenclature proposed previously[15] for systems derived from charged aromatic perimeters is less satisfactory in that the subscript labels the states merely by their energy order and contains no information on polarization directions.

The S, D, N_α, N_β, P_α, and P_β labels used for the excited states of nonaromatic perimeters are even less satisfactory in this regard, since the state labels cannot be deduced from a measurement of transition energies, intensities, and polarization directions alone. Either energy order (Figure 2) and either set of polarization directions is possible within the N and P state pairs: when the orbitals h_+ and s_+ have the same (opposite) symmetry, the transitions into the states labeled α (β) are polarized in the symmetry plane, and the transitions into the states labeled β (α) are polarized perpendicular to this plane. When two symmetry planes perpendicular to the molecular plane are present ($n = 4I$, where *I* is an integer), the situation is even worse since the attribution of the labels α and β then depends on which of the two symmetry planes is chosen for classification purposes.

We now propose that in all cyclic π-electron systems derived from a single perimeter, aromatic or nonaromatic, that contain a plane of symmetry perpendicular to the molecular plane, the subscript a *be used for states with transition moment for excitation from the ground state directed through one or two perimeter atoms, and the subscript* b *be used for those with this transition moment cutting only across bonds.* The only exception are aromatic or nonaromatic systems with $n = 4I$ and two mutually perpendicular planes of symmetry perpendicular to the molecular plane, since for these, both states would have the same label. In this instance, labels 1 and 2 in the order of increasing energy are the best we can offer.

In systems of lower symmetry, the states labeled a and b are mixed to some degree, and labels a or b should be associated with those states in which the a or b wave functions of the higher symmetry parent dominate; there will be cases in which the mixing is approximately 1:1 and in which the labels a and b will lose all significance.

Conclusion

Algebraic expressions for the energies, intensities, polarizations, and MCD signs of transitions into the low-lying singlet electronic states of unaromatic and ambiaromatic molecules derived from 4*N*-electron [*n*]annulene perimeters by structural perturbations such as cross-linking, bridging, substitution, and heteroatom replacement have been obtained from the perimeter

model for molecules containing at least one plane of symmetry perpendicular to the molecular plane. In its absence, perturbation theory can be applied to the results, most likely still producing useful qualitative insight.

For unaromatic and ambiaromatic systems derived from a 4*N*-electron perimeter, the perimeter model predicts the presence of six excited singlet states at relatively low energies. They cannot be simply correlated with the electronic states of the unperturbed antiaromatic parent perimeter. Two of the excited states of the unaromatic and ambiaromatic molecules arise from intrashell electron promotions: an electric-dipole-forbidden, magnetic-dipole-allowed S state, and a forbidden doubly excited D state. The other four arise from intershell promotions and carry electric-dipole intensity. Two weaker transitions are into the N_α and N_β states, and two stronger ones are into the P_α and P_β states. The N and P states are somewhat analogous to the familiar L and B states of systems derived from aromatic $(4N + 2)$-electron perimeters, respectively.

While the perimeter model predicts zero intensity for transitions to the S and D states, and thus provides no information on their polarization and MCD signs, it does provide such information for the four N and P states. The predicted spectral properties are simple functions of the orbital energy differences induced by the perturbation of the parent 4*N*-electron perimeter, which can be readily derived from low-level MO calculations and often by mere inspection of molecular formulas, as discussed in some detail in part 4 of this series. The concept of hard and soft MCD chromophores, familiar from the aromatic series, is applicable for unaromatic and ambiaromatic molecules as well.

Since perimeter model results are now available for all types of even-electron π-electron systems derived from a single perimeter that possess at least one plane of symmetry perpendicular to the molecular plane, we have proposed a generalization of the original Platt state labels that provides maximum immediate information about the relative energy, intensity, and polarization directions of transitions from the ground state. In molecules of lower symmetry, the a and b states mix to some degree, but the nomenclature remains useful in most cases.

Acknowledgment. This work was supported by a grant from the National Science Foundation (CHE-9819179). J.F. and U.H. are grateful to the Deutsche Forschungsgemeinschaft for scholarships, and J.F. acknowledges support by the Fonds der Chemischen Industrie.

References and Notes

(1) Part 2: Fleischhauer, J.; Höweler, U.; Michl, J. *Spectrochim. Acta* **1999**, *55*, 585.

(2) Platt, J. R. *J. Chem. Phys.* **1949**, *17*, 484. Moffitt, W. *J. Chem. Phys.* **1954**, *22*, 320, 1820.

(3) Michl, J. *J. Am. Chem. Soc.* **1978**, *100*, 6801.

(4) Michl, J. *J. Am. Chem. Soc.* **1978**, *100*, 6812.

(5) Michl, J. *J. Am. Chem. Soc.* **1978**, *100*, 6819.

(6) Höweler, U.; Chatterjee, P. S.; Klingensmith, K. A.; Waluk, J.; Michl, J. *Pure Appl. Chem.* **1989**, *61*, 2117.

(7) For an earlier discussion of the nature of electronic excitation in π systems derived from 4*N*-electron perimeters, see: Wirz, J. In *Excited States in Organic Chemistry and Biochemistry*; Pullman, B., Goldblum, N., Eds.; D. Reidel Publishing Co.; Dordrecht, Holland, 1977; p 283.

(8) Part 1: Höweler, U.; Downing, J. W.; Fleischhauer J.; Michl, J. *J. Chem. Soc., Perkin Trans.* **1998**, *2*, 1101, 2323.

(9) Part 4: Fleischhauer, J.; Michl, J. *J. Phys. Chem. A* **2000**, 7776.

(10) Kenney, J. W., III; Herold, D. A.; Michl, J. *J. Am. Chem. Soc.* **1978**, *100*, 6884.

(11) Parr, R. G. *J. Chem. Phys.* **1952**, *20*, 239.

(12) Dewar, M. J. S.; Dougherty, R. C. *The PMO Theory of Organic Chemistry*; Plenum: New York, 1975.

(13) Bonačić-Koutecký, V.; Koutecký, J.; Michl, J. *Angew. Chem., Int. Ed. Engl.* **1987**, *26*, 170.

(14) Schatz, P. N.; McCaffery, A. J. *Q. Rev. Chem. Soc.* **1969**, *23*, 552.

(15) Michl, J. *Tetrahedron* **1984**, *40*, 3845.

(16) Klessinger, M.; Michl, J. *Excited States and Photochemistry of Organic Molecules*; VCH Publishers: New York, 1995; Chapter 3.